ELECTRONIC TRANSITIONS IN THIOCARBONYL DICHLORIDE

ELECTRONIC TRANSITIONS
IN THIOCARBONYL DICHLORIDE

by

EDWARD ROBERT FARNWORTH, B.Sc.

A Thesis

Submitted to the Faculty of Graduate Studies

in Partial Fulfilment of the Requirements

for the Degree

Master of Science

McMaster University

July 1972

MASTER OF SCIENCE (1972)
(Chemistry)

McMASTER UNIVERSITY
Hamilton, Ontario

TITLE: Electronic Transitions in Thiocarbonyl Dichloride

AUTHOR: Edward Robert Farnworth, B.Sc. (Brock University)

SUPERVISOR: Dr. G. W. King, Dr. D. C. Moule

NUMBER OF PAGES: (viii), 110

SCOPE AND CONTENTS:

Calculations have been done for H_2CO, F_2CO, $C\ell_2CO$, H_2CS, F_2CS and $C\ell_2CS$, to determine the transition energy and oscillator strength of the $^1A_2 \leftarrow {}^1A_1(n \rightarrow \pi^*)$, $^1A_1 \leftarrow {}^1A_1(\pi \rightarrow \pi^*)$, $^1B_2 \leftarrow {}^1A_1(n \rightarrow \sigma^*)$ and $^1B_1 \leftarrow {}^1A_1(\sigma \rightarrow \pi^*)$ transitions. Eigenvalues were obtained from CNDO programs and used to calculate the oscillator strength at three levels of approximation.

The $^1A_1 \leftarrow {}^1A_1(\pi \rightarrow \pi^*)$ transition of $C\ell_2CS$ has been analysed. Four ground state and three excited state frequencies were found. Coon's method was used to establish the assignment and predict an excited state bent out of plane by 26.6°.

A previously unassigned transition in $C\ell_2CS$ has been labelled as $A_2 \leftarrow {}^1A_1(n \rightarrow \pi^*)$, on the basis of CNDO calculations, and five ground state frequencies have been found in the spectrum.

To my parents.

A small reward for a lifetime of

love and encouragement.

ACKNOWLEDGEMENTS

I would first like to thank Dr. G. W. King and Dr. D. C. Moule, my two supervisors. My only regrets are that I did not have the time to provide them with the level of work to which they are accustomed, and that they did not have the time to inspire me to the level of work of which I know I am capable.

Mr. M. Danyluk, Mr. E. Finn, Mrs. D. Grangé, Mr. F. Greening, Dr. G. Kidd, Mr. R. Lemanczyk, Mr. R. McLean, Mr. R. Meatherall, Mr. A. Van Putten, and Mr. C. R. Subramaniam: as colleagues, I am indebted to them. As friends, I will always remember them.

Mr. J. Bradford - very often used, very seldom thanked. The labours of Miss Susan Hawley (typing) and Mr. D. McEntee (printing) are much appreciated.

For two years you have been a part of me. Come, Lina, let's explore the world together.

TABLE OF CONTENTS

LIST OF TABLES

LIST OF FIGURES

CHAPTER 1

HISTORICAL INTRODUCTION

Thiocarbonyl dichloride was first prepared by Kolbe[1] in 1843 by the action of chlorine on carbon disulphide. It was not until 1925[2], however, that the first spectroscopic studies were carried out on $C\ell_2CS$. Henri then remarked on the similarities between the electronic spectrum of phosgene ($C\ell_2CO$) and the thiophosgene or thiocarbonyl dichloride ($C\ell_2CS$) spectrum. He was able to distinguish three electronic transitions. Two transitions were in the ultra-violet and one was in the visible region of the spectrum.

In the visible system, he was able to measure the wavelengths of five hundred bands between 3989.5 Å and 5711.8 Å. Three active frequencies were found: 911 cm^{-1}, 239 cm^{-1}, and 140 cm^{-1}. The 140 cm^{-1} vibration was assigned to motion involving the two chlorines, while the other two were attributed to activity in the thiocarbonyl group.

In the ultra-violet between 3280 Å and 2710 Å, four hundred bands were found. The bands were not as sharp as in the visible system, and so the spectrum was attributed to a "first state of predissociation".

The third system was below 2710 Å. Because of the diffuseness of the spectrum to the ultra-violet, it was concluded that this system was predissociated. He quoted the electronic activation energy for predissociation as being 105 kcal./gr.mole.

In 1938 H.W. Thompson[3] recorded the Raman spectrum of $C\ell_2CS$, using the exciting frequency 5876 Å. The following frequency intervals (in cm^{-1}) and relative intensities (in brackets) were found: 200(1), 287(3), 363(1), 496(5), 660(0), 1121(10), 1388(2). By analogy with phosgene[4], Thompson

was able to make the following assignments (the notation is the same as appears in Fig. 1.1): ν_1 = 1121 cm^{-1}, ν_2 = 496 cm^{-1}, ν_3 = 287 cm^{-1}, ν_4 = 660 cm^{-1}, ν_5 = 363 cm^{-1}, ν_6 = 200 cm^{-1}. The Raman interval 1388 cm^{-1} was attributed to a combination of ν_3 and ν_1.

In 1939 Henri and Duchesne[6] attempted to analyse the visible system of $C\ell_2CS$. They assumed that the ground state was planar, and thus could be assigned to the C_{2v} point group.

By 1956, two additional studies of $C\ell_2CS$ in the visible and ultraviolet had been undertaken[5,7]. The results of Duchesne and Burnelle's work are tabulated in Table 1.1. Burnelle also measured oscillator strengths for the electronic transitions of $C\ell_2CS$ dissolved in n-hexane. The intensity of the 5750-3900 Å system was reported as being $f = 1.26 \times 10^{-4}$, while the 2770-2390 Å system, localized in the $CC\ell_2$ group, had an oscillator strength of 10^{-1}.

Up to 1965 seven studies had been made on the infrared and force constants of $C\ell_2CS$, and attempts had been made to assign the six ground state frequencies[8-14]. Subsequently Brand et al.[15], from infrared spectroscopy, assigned the six frequencies as: ν_1 = 1139 cm^{-1}, ν_2 = 502 cm^{-1}, ν_3 = 292 cm^{-1}, ν_4 = 471 cm^{-1}, ν_5 = 818 cm^{-1}, ν_6 = 292 cm^{-1}, and these assignments are commonly accepted. Fig. 1.1 illustrates the six normal vibrations of $C\ell_2CS$.

Brand et al.[15] assigned the origin of the $^1A_2 \leftarrow {}^1A_1(n \rightarrow \pi^*)$ system as being "near" 18716.3 cm^{-1}. On the basis of Franck-Condon calculations, it was concluded that the excited state was similar to the analogous state of formaldehyde - that is, pyramidal - with an out of plane angle (θ) of 32°. These authors used in their calculations the ground state CS bond distance given by Brockway et al.[12] but transferred the $CC\ell$ and $C\ell$-C-$C\ell$ values from phosgene[81]. They also were able to identify in the U.V. spectrum five out of the six fundamental frequencies in the ground state, and also identified four excited state

Table 1.1

Analysis of the $C\ell_2CS$ Absorption Spectrum

by Duchesne and Burnelle

Spectral Region (Å)	ν_{0-0} (cm^{-1})	Transition[1]	Excited State[2]	Excited State Frequencies (cm^{-1})
~7000-5300	~15000	$^3\pi^* \leftarrow n$	$^3A_2(\pi^*,n)$	300 (unassigned) $\nu_2 = 400$
5750-3900	17344	$^1\pi^* \leftarrow n$	$^1A_2(\pi^*,n)$	$\nu_1 = 914, \nu_2 = 423$ $\nu_3 = 240, \nu_4 = 610$ $\nu_5 = ?\ , \nu_6 = 365$
2970-2690	33380±568	$\sigma^* \leftarrow n$ (localized in CS)	$^1A_2(\pi^*,n)$	$\nu_2 = 468, \nu_3 = 310$
2770-2390	36045	$\sigma^* \leftarrow n$ (localized in $CC\ell_2$)	$^1A_1(\pi^*,\pi)$	$\nu_2 = 442, \nu_3 = 208$

[1]Duchesne and Burnelle's assignments and symbolism.

[2]Modern assignments and symbolism, see text. The electronic ground state has $^1A_1$ symmetry under the C_{2v} point group.

Fig. 1.1

Normal Vibrations of $C\ell_2CS$

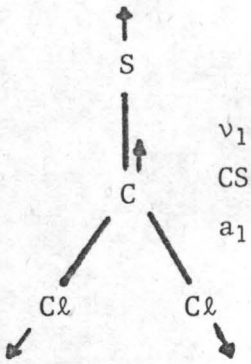

ν_1 = 1139 cm^{-1}
CS stretch
a_1 symmetry

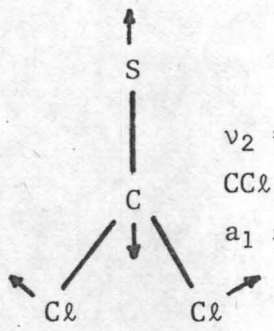

ν_2 = 502 cm^{-1}
$CC\ell$ stretch
a_1 symmetry

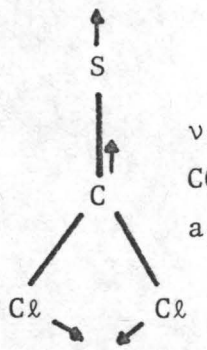

ν_3 = 292 cm^{-1}
$CC\ell_2$ bend
a_1 symmetry

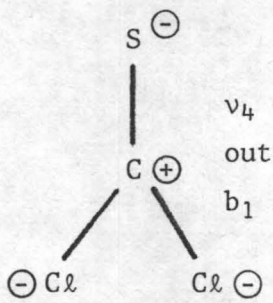

ν_4 = 471 cm^{-1}
out of plane bend
b_1 symmetry

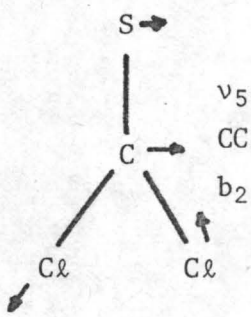

ν_5 = 818 cm^{-1}
$CC\ell$ stretch
b_2 symmetry

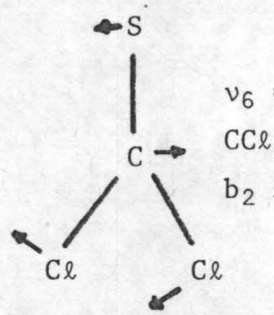

ν_6 = 292 cm^{-1}
$CC\ell_2$ rock
b_2 symmetry

frequencies. It was found that when the fundamentals formed progressions, the members exhibited an isotope effect.

Moule and Subramaniam[16] assigned the origin of the $^3A_2 \leftarrow {}^1A_1(n \rightarrow \pi^*)$ transition as occurring at 17492.0 cm^{-1}. Five of the six possible excited state frequencies were identified. Calculations on the potential barrier showed that the barrier to inversion of the pyramidal structure through the planar intermediate structure (see Chapter 4) was, for the $^1A_2$ state, 598 cm^{-1}, and 717 cm^{-1} for the $^3A_2$ state.

In 1967 Fabian, Viola and Meyer[17] studied more than sixty thiocarbonyl compounds. By semi-empirically defining a parameter "a" for each substituent of the thiocarbonyl group, they were able to predict the band maximum of the $A_2 \leftarrow {}^1A_1(n \rightarrow \pi^*)$ and $^1A_1 \leftarrow {}^1A_1(\pi \rightarrow \pi^*)$ transitions. They calculated that the $\pi^* \leftarrow \pi$ transition of $C\ell_2CS$ should occur at 2500 Å. They reported an experimental maximum at 2600 Å for $C\ell_2CS$ dissolved in cyclohexane.

In 1970 this author[18] confirmed the results of Fabian et al. and also measured the oscillator strengths of the $^1A_1 \leftarrow {}^1A_1(\pi^* \rightarrow \pi^*)$ transition in solution and gas phase (see Table 2.2). A transition to the red of the $^1A_1 \leftarrow {}^1A_1$ transition was also recorded, but was not identified.

The present work was undertaken to attempt a vibrational analysis of the $^1A_1 \leftarrow {}^1A_1(\pi^* \rightarrow \pi^*)$ system. It was hoped also that an excited state geometry could be determined. It was felt that through CNDO studies and oscillator strength calculations, that the unknown system could be identified and perhaps analysed.

CHAPTER 2

OSCILLATOR STRENGTHS

Introduction

In molecules, the electronic, vibrational and rotational energy levels are quantized. In electronic spectroscopy, the energies of vibrational and rotational transitions which accompany an electronic transition are measured. The basic theory is not described here; it is to be found in various text books[25,34,73]. An electronic transition is characterized by two properties, namely its energy and intensity. The energy of the transition, which is the difference in energy between the combining electronic states, can be expressed in familiar energy units such as electron volts (eV.), but is more commonly expressed in reciprocal centimetres (cm^{-1}), which are wavenumber units. The relation between the energy and the wavenumber is given by:

$$E = hc\sigma \qquad [2.1]$$

where h is Planck's constant;

c is the speed of light; and

σ is the wavenumber of the transition.

An electronic transition is composed of bands due to accompanying changes in the vibrational energy of the molecule. Each vibrational band is composed of transitions between individual rotational levels, producing lines which are often unresolved spectroscopically. Hence the total intensity of the electronic transition is the sum of the intensities of the vibrational bands.

The intensity of a band, or the totality of bands comprising an electronic transition, is commonly measured in two ways. Firstly the intensity can be described by the maximum value of the molar extinction coefficient ε_{max},

where ε is defined by[19,20]:

$$\log(I_o/I_n) = k\varepsilon n \qquad [2.2]$$

where I_o is the intensity of incident light;

I_n is the light intensity transmitted by the absorbing medium;

n is the path length; and

k is the concentration (in moles/cm^3).

ε_{max} is, however, only an approximate measure of the intensity of the transition itself, because the extinction coefficient is a function of the slit width, and resolving power of the spectrometer, and the nature of the solvent (if used). Also (and of more importance) under low resolution, different bands have different profiles. To overcome these difficulties the integrated intensity A[21] is often used to express the intensity of an electronic transition where:

$$A = \int_{\nu_1}^{\nu_2} \varepsilon_\nu d\nu \qquad [2.3]$$

where ε_ν is the molar extinction coefficient at the wavenumber ν; and

ν_1, ν_2 are the lower and upper frequency limits of the electronic transition.

The integrated intensity, then, is the area under the vibrational band envelope. It follows from equation [2.2] that A will have units of $\ell.mole.^{-1}cm.^{-2}$ The integrated intensity is used to calculate the more familiar oscillator strength f, for the electronic transition. The relation between the two is given by:

$$f = (10^3 \ln 10)\frac{mc^2}{\pi e^2 N} \int_{\text{all bands}} \int_{\nu_1}^{\nu_2} \varepsilon_\nu d\nu \qquad [2.4]$$

where m is the mass of the electron;

e is electronic charge; and

N is Avogadro's number.

The term band envelope of an electronic transition used here refers to the total intensity of the transition which consists of individual vibrational bands (which may or may not be resolved).

Oscillator Strengths

Consider a system with two electronic energy levels i, j (with $E_j > E_i$). When the system is placed in a field of electromagnetic radiation, the transition $j \leftarrow i$ can have a non-zero probability of occurrence[22,23]. In a time interval dt, the probability that the system will absorb radiation to induce the transition $j \leftarrow i$ is given by:

$$B_{ij} = \frac{2\pi}{3\hbar^2} |\tilde{R}|^2 \qquad [2.5]$$

where $\hbar = h/2\pi$; and

$\tilde{R}$ is called the transition moment.

The quantity $|\tilde{R}|^2$ is called the transition probability (see later), and can be decomposed into vector components:

$$|\tilde{R}|^2 = |\tilde{R}_x|^2 + |\tilde{R}_y|^2 + |\tilde{R}_z|^2 \qquad [2.6]$$

where $\tilde{R}_x$, $\tilde{R}_y$, $\tilde{R}_z$ are the x, y and z components of the transition moment. The oscillator strength of the transition $j \leftarrow i$ is given by[34]:

$$f_{j \leftarrow i} = \frac{4\pi mc\sigma |\tilde{R}|^2}{3he^2} \qquad [2.7]$$

where σ is the transition energy in cm^{-1}.

If σ is known, f is determined by $|\tilde{R}|^2$ since all other quantities in equation [2.7] are constants.

The Transition Moment[24]

The transition moment is expressed exactly as:

$$\tilde{R} = \int \psi_i |\tilde{M}| \psi_j d\tau \qquad [2.8]$$

where Ψ_i, Ψ_j are the total wavefunctions used to describe the initial and final states of the transition;

$\tilde{M}$ is the dipole moment operator; and

$d\tau$ is the product of the volume elements of the co-ordinates of the electrons and nuclei.

If Ψ_i and Ψ_j are known, an exact value can be calculated for the oscillator strength. Since they cannot be expressed in closed form, and in order to facilitate the calculations of f, a series of approximations are made.

(a) Rotational and vibrational contributions need not be considered, if the functions are expressed in terms of a molecule fixed co-ordinate system which rotates and vibrates with the molecule. Then the total wave function Ψ is reduced to an electronic wave function:

$$\Psi_{evr} = \psi_e(q,Q) \qquad [2.9]$$

where q are the electron co-ordinates; and

Q are the nuclear co-ordinates.

The dipole moment itself is made up of contributions from the electrons ($\tilde{M}_e$) and the nuclei ($\tilde{M}_n$), so that:

$$\tilde{M} = \tilde{M}_n + \tilde{M}_e \qquad [2.10]$$

Thus the transition moment in equation [2.8] can be rewritten in the form:

$$\tilde{R} = \int \Psi_i |\tilde{M}| \Psi_j d\tau$$

$$= \int \psi_{ei} |\tilde{M}_e| \psi_{ej} d\tau_e$$

where $d\tau_e$ is the product of the volume elements of the electronic co-ordinates.

(b) The electronic wave functions ψ_e are constructed from a basis set consisting of single electron atomic orbitals in linear combinations.

$$\psi_{e_i} = \sum_{t'=1}^{N} \sum_{\mu=1}^{n} \sum_{\alpha=1}^{n} C_\alpha \phi_{\mu t'} \qquad [2.13]$$

$$\psi_{e_j} = \sum_{t=1}^{N} \sum_{\nu=1}^{n} \sum_{\beta=1}^{n} C_\beta \phi_{\nu t}$$

where μ,ν label the type of orbitals in the basis set (1s, 2s, $2p_x$, etc.);

t, t' label the nuclear centre;

n is the number of orbitals used in the basis set; and

N is the number of nuclear centres.

In this work the same set of orbitals was used for the basis sets ϕ_μ, ϕ_ν. In the calculations carried out here, Slater type atomic orbitals were used[26]. Thus the initial and final states of the transition were described by linear combinations of the same atomic orbitals, but with different weighting factors. Also both combining states were assumed to have the same geometry.

(c) The electronic transition from i to j is considered to result from the promotion of a single electron, except when configuration interaction was used to determine the transition energy (see Appendix A).

Jaffé and Orchin[24] commented that the first and third assumptions are not as valid as the second, but the three assumptions allow one to rewrite equation [2.8] in a more useful form:

$$\tilde{R} = \int \sum_{t=1}^{N} \sum_{\nu=1}^{n} \sum_{\alpha=1}^{n} C_\alpha \phi_{\nu t} |\tilde{M}| \sum_{t'=1}^{N} \sum_{\mu=1}^{n} \sum_{\beta=1}^{n} C_\beta \phi_{\mu t'} d\tau \qquad [2.14]$$

Equation [2.14] can be decomposed into three equations, due to the form of the dipole moment operator. Since, by definition, the dipole moment is $e\tilde{r}$, in cartesian co-ordinates there are three components:

$$e\tilde{r} = e\tilde{x} + e\tilde{y} + e\tilde{z} \qquad [2.15]$$

Thus the x component of the transition moment can be written as:

$$\tilde{R}_x = \int \sum_{t=1}^{N} \sum_{\nu=1}^{n} \sum_{\alpha=1}^{n} C_\alpha \phi_{\nu t} |e\tilde{x}| \sum_{t'=1}^{N} \sum_{\mu=1}^{n} \sum_{\beta=1}^{n} C_\beta \phi_{\mu t'} d\tau \qquad [2.16]$$

It can be seen from equations [2.14] and [2.16] that the number of integrals that have to be calculated could be large, depending upon the size of the basis set. Further study of equation [2.14] will show how many of these integrals can be eliminated.

Selection Rules for Electronic Transitions

The transition moment may be zero for a given electronic transition. If this is the case, then the transition is said to be formally forbidden, but if the transition moment integral has a non-zero value, the transition is said to be allowed.

The dipole moment operator is linear. The expression $\langle \phi_j | \tilde{M} | \phi_i \rangle$ can be rearranged:

$$\langle \phi_j | \tilde{M} | \phi_i \rangle = \langle \phi_i | \tilde{M} | \phi_j \rangle = \langle | \tilde{M} | \phi_i \phi_j \rangle \qquad [2.17]$$

According to the geometrical distribution of its nuclei, every molecule can be assigned to a particular symmetry point group. The molecular wave functions must transform like one of the irreducible representations of this point group under its different symmetry operators. It can be shown that for an integral of the type in equation [2.17], the integrand must transform like the totally symmetric representation of the molecular point group[27]. This provides selection rules which determine whether a transition between two states is allowed or not.

(a) If a molecule has a centre of symmetry, then all electronic wave functions, or functions constructed from a linear combination of wave functions are either symmetric or antisymmetric with respect to the centre of symmetry. If the wave function (or combination) is symmetric, it is called g (gerade or even), if

antisymmetric u (odd or ungerade). The x, y, z components of the dipole moment operator are u. In order that the transition moment integral not vanish, the integrand must be gerade. This can only result if the two electronic states are of opposite parity. Thus,

$$\begin{array}{lll} g \rightarrow u & & g \not\rightarrow g \\ & \text{but} & \\ u \rightarrow g & & u \not\rightarrow u \end{array} \qquad [2.18]$$

(b) The two non-degenerate electronic states ϕ_i and ϕ_j serve as bases for the representations $\Gamma\phi_i$ and $\Gamma\phi_j$ respectively, of the point group of the molecule. The components of the electric dipole moment operators $\tilde{M}_x$, $\tilde{M}_y$, $\tilde{M}_z$ also serve as bases for the representations $\Gamma\tilde{M}_x$, $\Gamma\tilde{M}_y$, $\Gamma\tilde{M}_z$. These transform like vectors along the x, y and z axes respectively. Then in order for the transition to be allowed, the direct product $\Gamma\phi_i \otimes \Gamma\phi_j$ must transform as one of the components of $\tilde{M}$. That is:

$$\Gamma\phi_i \otimes \Gamma\phi_j = \begin{cases} \Gamma\tilde{M}_x \\ \Gamma\tilde{M}_y \\ \Gamma\tilde{M}_z \end{cases} \qquad [2.19]$$

(c) The wave functions of each electronic state can be expressed in terms of a linear combination of ground state wave functions, which includes both space (ϕ) and spin (α,β) components. By taking the product of the one electron space orbitals and the one electron spin orbitals, spin-orbitals are formed. Each of these spin-orbitals can accommodate two electrons. Each electron in turn can have two possible spin states - α, β. According to the number of electrons, and the occupancy of the two possible spin states, the electronic state can be described as singlet, doublet, triplet, etc. If the i^{th} state is a singlet (say) it can be represented by $\phi_i\alpha\beta$. Now if the j^{th} state is a triplet, it will be represented by $\phi_j\alpha^2$ (the two other components would be

represented by $\phi_j\beta^2$ and $\phi_j[\alpha(1)\beta(2) + \alpha(2)\beta(1)]$). In this example then, the transition moment becomes:

$$\tilde{R} = \int \phi_i\alpha\beta|\tilde{M}|\phi_j\alpha^2 d\tau d\sigma \qquad [2.20]$$

where $d\tau$ is the product of the volume elements of the co-ordinates of the space part of the electronic wave function; and

$d\sigma$ is the product of the volume elements of the co-ordinates of the spin part of the electronic wave function.

The space and spin parts of equation [2.20] can be separated as:

$$\tilde{R} = \int \phi_i|\tilde{M}|\phi_j d\tau \int\alpha^3\beta d\sigma \qquad [2.21]$$

Obviously the second integral is odd and will be zero upon integration. Thus the transition is forbidden. This result is also true if the two other components of the triplet had been used. Hence the spin selection rules for transitions are:

singlet → singlet
triplet → triplet
but singlet ↛ triplet

CNDO Synthesis of Electronic States

The molecules considered in this thesis are H_2CO, F_2CO, $C\ell_2CO$, H_2CS, F_2CS, and $C\ell_2CS$. The CNDO method (complete neglect of differential overlap) was used to describe their electronic states. Two different program versions of this method were employed. The first program was obtained from the Quantum Chemistry Program Exchange and was written by Pople and Dobosh (hereafter it will be referred to as CNDO-PD). Its main advantage was that it could be used for molecules constructed from atoms up to and including chlorine. The second program was obtained from the Quantum Chemistry Program Exchange and was written by Del Bene and H. Jaffé[28] (hereafter it will be referred to as CNDO-JD). The most useful feature of this program was that it contained a

configuration interaction subroutine (see Appendix A) along with a simple oscillator strength calculation.

The input for these programs included the co-ordinates and atomic numbers of the various atoms comprising the molecule (and in the case of Jaffé's program, the symmetry of the molecule). The output included the total electronic energy, and the single-electron molecular orbitals, arranged in order of increasing energy, into which the valence electrons of the atoms comprising the molecule are fed. These molecular orbitals were constructed as linear combinations of atomic orbitals. In the CNDO programs, Slater type orbitals were used.

Thiocarbonyl dichloride was of primary interest experimentally, and so the oscillator strengths of $C\ell_2CS$ and its carbonyl and thiocarbonyl chromophores were studied. In the series of molecules H_2CO, F_2CO, $C\ell_2CO$, H_2CS, F_2CS and $C\ell_2CS$, theoretical answers were sought to the following questions: (a) Is there any difference between the oscillator strengths of carbonyl and thiocarbonyl compounds? (b) What is the effect of halogen substitution on the oscillator strength of these compounds? (c) Can an oscillator strength calculation tested on a well-known system (H_2CO) be used to make predictions as to the types of transitions which could occur in less understood spectra of molecules such as $C\ell_2CS$?

Experimentally it is known that H_2CO[29], F_2CO[30], $C\ell_2CO$[31], H_2CS[32] and $C\ell_2CS$[33] are of C_{2v} symmetry in the ground state. Also some experimental measurements have been made of the oscillator strengths of electronic transitions in these compounds. This information for the carbonyls is contained in Table 2.1[34,35]. Table 2.2 contains the information for the thiocarbonyls. All of the values in the tables have been previously reported in the literature, except for the f values of $C\ell_2CS$ for the $^1A_2 \leftarrow {}^1A_1(n \rightarrow \pi^*)$ and $^1A_1 \leftarrow {}^1A_1(\pi \rightarrow \pi^*)$

transitions, which have been measured by this investigator.

The calculations to follow will be compared to the values in Tables 2.1 and 2.2, and for this reason a closer analysis of the experimental data will prove useful. Several systems have been analysed to the point where the type of transition and the origin band of the transition are now known. Other systems have only been recorded experimentally and speculation made as to their nature.

Formaldehyde (H_2CO) has served as a model for all the other compounds, in terms of spectroscopic analysis. The $^{1,3}A_2 \leftarrow {}^1A_1(n \rightarrow \pi^*)$ transitions have been studied extensively, but as yet two values are quoted by Hertzberg[73] for the origin of the $^3A_2 \leftarrow {}^1A_1(n \leftarrow \pi^*)$ transition.

The overlap of the 0-0 band with nearby bands in the $^1A_2 \leftarrow {}^1A_1(n \rightarrow \pi^*)$ system leads also to two values for the origin. Brand[38] quoted 28196 cm^{-1} while Callomon and Innes[83] reported the 0-0 band as being centred at 28188 cm^{-1}. This latter value was checked by analysing the rotational structure and thus can be assumed to be more reliable than Brand's value. The oscillator strengths were evaluated by DiGiorgio and Robinson[36] on the assumption that the $^3A_2 \leftarrow {}^1A_1(n \rightarrow \pi^*)$ was 0.005 times as intense as the $^1A_2 \leftarrow {}^1A_1(n \rightarrow \pi^*)$ system. They quoted Duncan and House's value of $f = 2.4 \times 10^{-5}$[84] for the $^1A_2 \leftarrow {}^1A_1(n \rightarrow \pi^*)$ system, and calculated that the $^3A_2 \leftarrow {}^1A_1(n \rightarrow \pi^*)$ oscillator strength was $f = 1.2 \times 10^{-6}$. They attached an error of a factor of two to the triplet value. Fleming et al.[41] studied the H_2CO spectrum in the 1750 Å region. On the basis of calculations carried out by Pople and Sidman[85] they assigned the transition as $^1B_2 \leftarrow {}^1A_1(n \rightarrow \sigma^*)$. The lowest energy band maximum occurred at 57180±20 cm^{-1}. An oscillator strength of $f = 0.04$ was measured, as the area under the experimental curve between 56500 and 63000 cm^{-1}. Price[40] recorded a system of diffuse bands for H_2CO. The lowest energy member of this

system came at 64270±50 cm^{-1}. Price did not speculate as to the nature of the system. Herzberg[73] has assigned the transition as being $^1A_1 \leftarrow {}^1A_1(\pi \rightarrow \pi^*)$. Although he quotes Price's work he gives 64264 cm^{-1} as the T_o value. King[40] on the basis of comparative spectra quotes an oscillator strength value for this transition as f = 0.1 - 0.5.

Workman and Duncan[42] studied the spectra of F_2CO down to 1215 Å. They reported two overlapping systems which they assigned as $A_2 \leftarrow {}^1A_1(n \rightarrow \pi^*)$ transitions because of their intensity and similarity in vibrational structure. The first system extended from 42084 cm^{-1} to 56000 cm^{-1}. Its oscillator strength was given as $f = 3 \times 10^{-4}$. These workers stated that the energy values were accurate to ±10 cm^{-1}, while their oscillator strength values were good to ±10-20%. The second $A_2 \leftarrow {}^1A_1(n \rightarrow \pi^*)$ system overlapped the first but Workman and Duncan stated that this transition began at 56000 cm^{-1} and extended to 61800 cm^{-1} with a maximum in intensity at 59200 cm^{-1}. In their table of frequencies for this transition they gave the lowest energy band an energy of 56598 cm^{-1}. By extrapolating the two $A_2 \leftarrow {}^1A_1(n \rightarrow \pi^*)$ transitions into each other they were able to measure the oscillator strength of the second system as $f = 5 \times 10^{-4}$. A third transition beginning at 65597 cm^{-1} and extending to 68711 cm^{-1} consisted of only five broad bands. The oscillator strength was measured and because of the high value (1×10^{-3}) they concluded that the transition was allowed. The transition was assigned as $B_1 \leftarrow {}^1A_1(\sigma \rightarrow \pi^*)$. A fourth system slightly overlapped the third. It was a continuous absorption with a maximum at approximately 76000 cm^{-1}. The large oscillator strength (f = 0.15) and the energy of the transition led to the conclusion that the transition was $^1A_1 \leftarrow {}^1A_1(\pi \rightarrow \pi^*)$.

Moule and Foo[43] were able to assign a band at 33631.2 cm^{-1} as a false origin - 4_0^1, of the $^1A_2 \leftarrow {}^1A_1(n \rightarrow \pi^*)$ transition in $C\ell_2CO$. The origin band

transition is formally forbidden in the $^{1,3}A_2 \leftarrow {}^1A_1(n \rightarrow \pi^*)$ transitions and so a false origin may be observed rather than the true origin. The assignment was made by making use of low temperature spectra, and by fitting the observed progressions in ν_4'' and ν_4' to calculated progressions. The oscillator strength was measured from the integrated area under the absorption band recorded by a Cary Model 14 Spectrophotometer.

Moule and Mehra[44] in an analogous manner assigned 23477.1 cm^{-1} as the false origin 4_0^1 of the $^1A_2 \leftarrow {}^1A_1(n \rightarrow \pi^*)$ transition in F_2CS. The $^3A_2 \leftarrow {}^1A_1(n \rightarrow \pi^*)$ was also studied by Moule[45]. Progressions in ν_4' and ν_2' converged on a common band at 22191.1 cm^{-1} which was assigned as the origin of the transition. The oscillator strength of the singlet system has been recently measured by C. Drury. The value was given as $f = 9.8 \times 10^{-5}$[46]. Fabian, Viola and Meyer[17] in their paper on semi-empirical calculations of thiocarbonyls, quoted the experimentally determined band maximum for the $^1A_1 \leftarrow {}^1A_1(\pi \rightarrow \pi^*)$ transition in F_2CS as occurring at 49000 cm^{-1}. C. Drury[46] has estimated the origin of the transition to be approximately 39570 cm^{-1}. She has also measured the oscillator strength as being $f = 0.24$.

Brand et al.[33] analysed in great detail the $^1A_2 \leftarrow {}^1A_1(n \rightarrow \pi^*)$ system of $C\ell_2CS$. They assigned the band at 18716.28 cm^{-1} as the false origin 4_0^1. The assignment was supported by isotope data, and comparison to the H_2CO $^1A_2 \leftarrow {}^1A_1(n \rightarrow \pi^*)$ system. The $^3A_2 \leftarrow {}^1A_1(n \rightarrow \pi^*)$ system was studied by Moule and Subramaniam[16]. They found that progressions in ν_1', ν_2', ν_3' and ν_4' all converged on a band at 17492.0 cm^{-1} which they assigned as the electronic origin. The oscillator strength for the $^1A_2 \leftarrow {}^1A_1(n \rightarrow \pi^*)$ system was measured by this investigator from a gas phase spectrum recorded using a Cary Model 14 spectrophotometer. Fabian et al.[17] in their paper on thiocarbonyls also predicted and measured the band maximum for the $^1A_1 \leftarrow {}^1A_1(\pi \rightarrow \pi^*)$ system of

$C\ell_2CS$ dissolved in cyclohexane. They reported the maximum to occur at 38500 cm^{-1}. This investigator recorded the gas phase spectrum and found the maximum to occur at 39793 cm^{-1}. The oscillator strength of the system was also measured in both cyclohexane and the gas phase. The gas phase value was a factor two less than the cyclohexane value.

Two points should be made before proceeding. Firstly, in many cases the 0-0 band or false origin has been assigned experimentally. However, in the calculations that will be compared to these experimental results, it is the energy of the band maximum that will be calculated. The band maximum and the origin can, in many cases, differ significantly. A comparison of calculated values and experimental energies should be made in this light. Secondly, the values of the oscillator strengths are quoted with no indication as to the magnitude of the uncertainty of the values (with one exception). Obviously the error will vary from system to system. Workman and Duncan's estimate of a 10-20% error for their values does not seem unreasonable however. (It has been this investigator's experience that such a magnitude error would be in many cases very conservative.) An exact correlation of calculated and experimental oscillator strength may be possible then, only within these limits.

The results from a CNDO program have been found to be very sensitive with respect to input geometry[48]. The input geometries used here are listed in Table 2.3. Whenever possible, values were taken from Herzberg's book: "Electronic Spectra of Polyatomic Molecules" (ref. 73). Also different basis sets were used to generate the molecular orbitals, depending upon whether the molecule contained first or second row elements. The basis sets used for the compounds studied are listed in Table 2.4.

The number of molecular orbitals obtained from the basis set is equal to the number of atomic orbitals comprising the basis set. Thus in the case

Table 2.1

Experimental Transition Energies and Oscillator Strengths of Some Carbonyls

	$A_2 \leftarrow {}^1A_1(n \rightarrow \pi^*)$	$^1A_1 \leftarrow {}^1A_1(\pi \rightarrow \pi^*)$	$^1B_2 \leftarrow {}^1A_1(n \rightarrow \sigma^*)$	$^1B_1 \leftarrow {}^1A_1(\sigma \rightarrow \pi^*)$
H_2CO				
E (cm^{-1})	25200.2[a] triplet (39) 25194 (82) 28188[b] singlet (83) 28196 (38)	64270±50[c] (40) 64264 (73)	57180±20[c] singlet (41)	-
f	1.2×10^{-6} triplet (36) 2.4×10^{-4} singlet (36)	~0.1 - 0.5 (34)	0.04 (41)	-
F_2CO (42)				
E (cm^{-1})	42084[c]-56000 first system 56598-61800(59200[e]) second system	76000[e]	65597[c]-68711	-
f	3×10^{-4} first system 5×10^{-4} second system	0.15	1×10^{-3}	-
Cl_2CO				
E (cm^{-1})	33631.2[d] singlet (43)	-	-	-
f	1.04×10^{-3} singlet (43)	-	-	-

[a] 0^+ level.

[b] 0-0 band centre.

[c] lowest energy band in system.

[d] false origin.

[e] band maximum.

NOTE: All oscillator strengths are for gas phase.

Table 2.2

Experimental Energies and Oscillator Strengths of Some Thiocarbonyls

	$A_2 \leftarrow {}^1A_1(n \rightarrow \pi^*)$	$^1A_1 \leftarrow {}^1A_1(\pi \rightarrow \pi^*)$	$^1B_2 \leftarrow {}^1A_1(n \rightarrow \sigma^*)$	$^1B_1 \leftarrow {}^1A_1(\sigma \rightarrow \pi^*)$
H_2CS				
E (cm^{-1})	-	-	-	-
f	-	-	-	-
F_2CS				
E (cm^{-1})	23477.1[a] singlet (44) 22191.1 triplet (45)	49000[b] (17) 39570[c] (46)	- -	- -
f	9.8×10^{-5} singlet (46)	0.24 (46)	-	-
$C\ell_2CS$			'unknown system'	
E (cm^{-1})	18716.28[a] singlet (33) 17492.0 triplet (47)	38500[b] (in cyclohexane) (17) 39793[b] (in gas phase) (18)	- -	~31100[b] (18) -
f	3.65×10^{-5} singlet (56)	1.01×10^{-1} (in cyclohexane) 5.90×10^{-2} (in gas phase)	- -	2.42×10^{-5} (18) -

[a] false origin.

[b] band maximum.

[c] probable origin.

NOTE: Oscillator strength values are for gas phase unless otherwise noted.

Table 2.3

Bond Lengths and Bond Angles Used in

CNDO Calculations

Carbonyls (X_2CO)

	R_{CO} (Å)	R_{CX} (Å)	∠ XCX	∠ out of plane
H_2CO (73)	1.210	1.102	121.1°	0.0
F_2CO (73)	1.174	1.312	108.0°	0.0
$C\ell_2CO$ (73)	1.166	1.746	111.3°	0.0

Thiocarbonyls (X_2CS)

	R_{CS} (Å)	R_{CX} (Å)	∠ XCX	∠ out of plane
H_2CS (79)	1.6108	1.0925	116.87°	0.0
F_2CS (80)	1.63	1.32	111.75°	0.0
$C\ell_2CS$ (15)	1.63	1.746	111.3°	0.0

Table 2.4

Basis Sets Used in CNDO Calculations

H_2CO: $1s_{H_1}$, $1s_{H_2}$, $2s_C$, $2s_O$, $2p_{x_C}$, $2p_{x_O}$, $2p_{y_C}$, $2p_{y_O}$, $2p_{z_C}$, $2p_{z_O}$

F_2CO: $2s_C$, $2s_O$, $2s_{F_1}$, $2s_{F_2}$, $2p_{x_C}$, $2p_{x_O}$, $2p_{x_{F_1}}$, $2p_{x_{F_2}}$, $2p_{y_C}$, $2p_{y_O}$, $2p_{y_{F_1}}$, $2p_{y_{F_2}}$, $2p_{z_C}$, $2p_{z_O}$, $2p_{z_{F_1}}$, $2p_{z_{F_2}}$

Cl_2CO: $2s_C$, $2s_O$, $2p_{x_C}$, $2p_{x_O}$, $2p_{y_C}$, $2p_{y_O}$, $2p_{z_C}$, $2p_{z_O}$, $3s_{Cl_1}$, $3s_{Cl_2}$, $3p_{x_{Cl_1}}$, $3p_{x_{Cl_2}}$, $3p_{y_{Cl_1}}$, $3p_{y_{Cl_2}}$, $3p_{z_{Cl_1}}$, $3p_{z_{Cl_2}}$, $3d_{z^2{}_{Cl_1}}$, $3d_{z^2{}_{Cl_2}}$, $3d_{xz_{Cl_1}}$, $3d_{xz_{Cl_2}}$, $3d_{yz_{Cl_1}}$, $3d_{yz_{Cl_2}}$, $3d_{x^2-y^2{}_{Cl_1}}$, $3d_{x^2-y^2{}_{Cl_2}}$, $3d_{xy_{Cl_1}}$, $3d_{xy_{Cl_2}}$

H_2CS: $1s_{H_1}$, $1s_{H_2}$, $2s_C$, $2p_{x_C}$, $2p_{y_C}$, $2p_{z_C}$, $3s_S$, $3p_{x_S}$, $3p_{y_S}$, $3p_{z_S}$, $3d_{z^2{}_S}$, $3d_{xz_S}$, $3d_{yz_S}$, $3d_{x^2-y^2{}_S}$, $3d_{xy_S}$

F_2CS: $2s_C$, $2s_{F_1}$, $2s_{F_2}$, $2p_{x_C}$, $2p_{x_{F_1}}$, $2p_{x_{F_2}}$, $2p_{y_C}$, $2p_{y_{F_1}}$, $2p_{y_{F_2}}$, $2p_{z_C}$, $2p_{z_{F_1}}$, $2p_{z_{F_2}}$, $3s_S$, $3p_{x_S}$, $3p_{y_S}$, $3p_{z_S}$, $3d_{z^2{}_S}$, $3d_{xz_S}$, $3d_{yz_S}$, $3d_{x^2-y^2{}_S}$, $3d_{xy_S}$

Cl_2CS: $2s_C$, $2p_{x_C}$, $2p_{y_C}$, $2p_{z_C}$, $3s_S$, $3s_{Cl_1}$, $3s_{Cl_2}$, $3p_{x_S}$, $3p_{x_{Cl_1}}$, $3p_{x_{Cl_2}}$, $3p_{y_S}$, $3p_{y_{Cl_1}}$, $3p_{y_{Cl_2}}$, $3p_{z_S}$, $3p_{z_{Cl_1}}$, $3p_{z_{Cl_2}}$, $3d_{z^2{}_S}$, $3d_{z^2{}_{Cl_1}}$, $3d_{z^2{}_{Cl_2}}$, $3d_{xz_S}$, $3d_{xz_{Cl_1}}$, $3d_{xz_{Cl_2}}$, $3d_{yz_S}$, $3d_{yz_{Cl_1}}$, $3d_{yz_{Cl_2}}$, $3d_{x^2-y^2{}_S}$, $3d_{x^2-y^2{}_{Cl_1}}$, $3d_{x^2-y^2{}_{Cl_1}}$, $3d_{xy_S}$, $3d_{xy_{Cl_1}}$, $3d_{xy_{Cl_2}}$

of H_2CO the CNDO program generated ten molecular orbitals, while for $C\ell_2CS$ thirty-one molecular orbitals resulted. Into these various molecular orbitals, the valence shell electrons were fed, and the molecular orbitals (σ, π, n, π^*, σ^*) were labelled according to their symmetries and energies.

The molecular orbitals having been obtained, the evaluation of the transition moment integrals by means of equation [2.16] should have been straight-forward. However, further approximations were found to be necessary.

Levels of Approximation in Oscillator Strength Calculations

Cusachs and Trus[49] state that "one centre integrals are few in number and easy to evaluate; they present neither practical nor theoretical difficulty". In the case of H_2CO this may be so, but for $C\ell_2CS$ where the number of atomic orbitals is thirty-one, their statement is unreasonable. Because of this, several approximations can be made to facilitate the evaluation of the relevant integral:

$$\tilde{R} = \int \sum_{t}^{N} \sum_{\nu}^{n} \sum_{\alpha}^{n} C_\alpha \phi_{\nu t} |\tilde{M}| \sum_{t'}^{N} \sum_{\mu}^{n} \sum_{\beta}^{n} C_\beta \phi_{\mu t'} d\tau \qquad [2.22]$$

In the expansion of equation [2.22], two types of terms will arise:

$$\tilde{U} = \int C_\alpha \phi_{\nu_t} |\tilde{M}| C_\beta \phi_{\mu_t} d\tau \qquad \text{where } t = t' \qquad [2.23]$$

$$\tilde{T} = \int C_\alpha \phi_{\nu_t} |\tilde{M}| C_\beta \phi_{\mu t'} d\tau \qquad \text{where } t' \neq t \qquad [2.24]$$

Since the t, t' label distinguishes atomic centres, integral [2.23] is termed a one-centre integral and integral [2.24] is called a two-centre integral. The first approximation is to ignore the two-centre contributions to the transition moment. The main justification for this[27] is that the magnitude of the two-centre integrals is much less (in most cases by an order of magnitude) than that of the one-centre integrals, and hence their contribution to the transition moment is less. Comparison of Table 2.5 and Table

2.6 verifies this assumption. Also evaluation of the two-centre integrals represents a problem in itself (see later).

Although the evaluation of the one-centre integrals presents little mathematical problem, an approximation that foregoes the formal integration can be introduced. This approximation can be termed the co-ordinate dependent method, and is the one used in the Jaffé CNDO program[50]. In the co-ordinate dependent method, expanded integrals of the type in equation [2.25] can be approximated by equation [2.26]:

$$\tilde{U} = \int C_\alpha \phi_{\nu_t} |\tilde{M}| C_\beta \phi_{\mu_t} d\tau = \int C_\alpha \phi_{\nu_t} |e\tilde{x}| C_\beta \phi_{\mu_t} d\tau + \int C_\alpha \phi_{\nu_t} |e\tilde{y}| C_\beta \phi_{\mu_t} d\tau + \int C_\alpha \phi_{\nu_t} |e\tilde{z}| C_\beta \phi_{\mu_t} d\tau \qquad [2.25]$$

$$= C_\alpha C_\beta \tilde{x} + C_\alpha C_\beta \tilde{y} + C_\alpha C_\beta \tilde{z} \qquad [2.26]$$

where $\tilde{x}$, $\tilde{y}$, $\tilde{z}$ are the Cartesian co-ordinates of atom t.

This approximation eliminates any integrations, but it retains an important feature of the transition moment. The integral $\tilde{R} = \int \Psi_i |\tilde{M}| \Psi_j d\tau$ (equation [2.8]) could be described in terms of a charge migration, i.e., a displacement of charge during the electronic transition from i to j[24]. Thus the magnitude of the transition moment (and the resulting oscillator strength) are related to the size of the molecule through $\tilde{M}$. The co-ordinate dependent method retains this relation between molecular size and the resulting oscillator strength.

A second level of approximation can be used whereby integrals of the type represented in equation [2.23] are explicitly evaluated. Since single-electron orbitals are used, and the integrals are one-centre, the transition moment integrals can be expressed in terms of only one variable - the Slater coefficient[26].

It follows from the symmetry selection rules that the only non-zero one-centre integrals are of the form:

$$\tilde{U} = \int C_\alpha \phi_{ns_t} |\tilde{M}| C_\beta \phi_{np_t} d\tau$$

and [2.27]

$$\tilde{U} = \int C_\alpha \phi_{mp_t} |\tilde{M}| C_\beta \phi_{md_t} d\tau$$

where n, m take the values 2, 3 since only 2s, 2p, 3s, 3p and 3d orbitals are used in the calculations.

It is realized that although integrals of the type:

$$\tilde{U} = \int C_\alpha \phi_{np_t} |\tilde{M}| C_\beta \phi_{np_t} d\tau \qquad [2.28]$$

are formally zero, the integrals are set to zero only if the atomic centre being considered is situated at the origin of the co-ordinate system. In all other cases, the integral is replaced by the square root of the sum of the squares of the Cartesian co-ordinates of the atomic centre being considered. In their work on aromatic hydrocarbons, Burnelle and Kranepool[51] made similar approximations.

Since the one-centre integrals are needed in both oscillator strength calculations and dipole moment calculations, the one-centre integral values for atoms carbon to chlorine are listed in Table 2.5.

The last level of approximation included two-centre integrals.

Two-Centre Moment Integral Evaluation

The two-centre integrals are of form:

$$\tilde{T} = \int C_\alpha \phi_{\nu_t} |\tilde{M}| C_\beta \phi_{\mu_{t'}} d\tau \qquad \text{where } t \neq t' \qquad [2.29]$$

where the orbitals considered are on two different (neighbouring) centres. As in the one-centre calculations, Slater-type orbitals of the form:

Table 2.5

One-Centre Moment Integrals

	Component		
	$\tilde{x}$ (eÅ)	$\tilde{y}$ (eÅ)	$\tilde{z}$ (eÅ)
Carbon			
$\int 2s \lvert\tilde{M}\rvert 2p_x d\tau$	.0000	.8882	.0000
$\int 2s \lvert\tilde{M}\rvert 2p_y d\tau$	.8882	.0000	.0000
$\int 2s \lvert\tilde{M}\rvert 2p_z d\tau$	.0000	.0000	.8882
Nitrogen			
$\int 2s \lvert\tilde{M}\rvert 2p_x d\tau$	.0000	.8108	.0000
$\int 2s \lvert\tilde{M}\rvert 2p_y d\tau$	.8108	.0000	.0000
$\int 2s \lvert\tilde{M}\rvert 2p_z d\tau$	.0000	.0000	.8108
Oxygen			
$\int 2s \lvert\tilde{M}\rvert 2p_x d\tau$	.0000	.7344	.0000
$\int 2s \lvert\tilde{M}\rvert 2p_y d\tau$	.7344	.0000	.0000
$\int 2s \lvert\tilde{M}\rvert 2p_z d\tau$	.0000	.0000	.7344
Fluorine			
$\int 2s \lvert\tilde{M}\rvert 2p_x d\tau$	.0000	.5552	.0000
$\int 2s \lvert\tilde{M}\rvert 2p_y d\tau$	.5552	.0000	.0000
$\int 2s \lvert\tilde{M}\rvert 2p_z d\tau$	.0000	.0000	.5552
Sulphur			
$\int 3s \lvert\tilde{M}\rvert 3p_x d\tau$	.0000	.7416	.0000
$\int 3s \lvert\tilde{M}\rvert 3p_y d\tau$	.7416	.0000	.0000
$\int 3s \lvert\tilde{M}\rvert 3p_z d\tau$	.0000	.0000	.7416
$\int 3p_x \lvert\tilde{M}\rvert 3d_{x^2-y^2} d\tau$	.2872	.0000	.0000
$\int 3p_x \lvert\tilde{M}\rvert 3d_{xz} d\tau$	.0000	.0000	.2872
$\int 3p_x \lvert\tilde{M}\rvert 3d_{z^2} d\tau$	.0000	.1658	.0000
$\int 3p_x \lvert\tilde{M}\rvert 3d_{yz} d\tau$	.0000	.0000	.0000
$\int 3p_x \lvert\tilde{M}\rvert 3d_{xy} d\tau$	.0000	.2872	.0000
$\int 3p_y \lvert\tilde{M}\rvert 3d_{x^2-y^2} d\tau$	.0000	.2872	.0000
$\int 3p_y \lvert\tilde{M}\rvert 3d_{xz} d\tau$	.0000	.0000	.0000

Table 2.5 (cont'd.)

	Component		
	$\tilde{x}$ (eÅ)	$\tilde{y}$ (eÅ)	$\tilde{z}$ (eÅ)
Sulphur			
$\int 3p_y \lvert\tilde{M}\rvert 3d_{z^2} d\tau$	.1658	.0000	.0000
$\int 3p_y \lvert\tilde{M}\rvert 3d_{yz} d\tau$	.0000	.0000	.2872
$\int 3p_y \lvert\tilde{M}\rvert 3d_{xy} d\tau$	.2872	.0000	.0000
$\int 3p_z \lvert\tilde{M}\rvert 3d_{x^2-y^2} d\tau$	.0000	.0000	.0000
$\int 3p_z \lvert\tilde{M}\rvert 3d_{xz} d\tau$	.0000	.2872	.0000
$\int 3p_z \lvert\tilde{M}\rvert 3d_{z^2} d\tau$	.0000	.0000	.3316
$\int 3p_z \lvert\tilde{M}\rvert 3d_{yz} d\tau$	.2872	.0000	.0000
$\int 3p_z \lvert\tilde{M}\rvert 3d_{xy} d\tau$	.0000	.0000	.0000
Chlorine			
$\int 3s \lvert\tilde{M}\rvert 3p_x d\tau$	.0000	.6626	.0000
$\int 3s \lvert\tilde{M}\rvert 3p_y d\tau$	.6626	.0000	.0000
$\int 3s \lvert\tilde{M}\rvert 3p_z d\tau$	.0000	.0000	.6626
$\int 3p_x \lvert\tilde{M}\rvert 3d_{x^2-y^2} d\tau$	.2566	.0000	.0000
$\int 3p_x \lvert\tilde{M}\rvert 3d_{xz} d\tau$	.0000	.0000	.2566
$\int 3p_x \lvert\tilde{M}\rvert 3d_{z^2} d\tau$	.0000	.1481	.0000
$\int 3p_x \lvert\tilde{M}\rvert 3d_{yz} d\tau$	.0000	.0000	.0000
$\int 3p_x \lvert\tilde{M}\rvert 3d_{xy} d\tau$	.0000	.2566	.0000
$\int 3p_y \lvert\tilde{M}\rvert 3d_{x^2-y^2} d\tau$	.0000	.2566	.0000
$\int 3p_y \lvert\tilde{M}\rvert 3d_{xz} d\tau$	.0000	.0000	.0000
$\int 3p_y \lvert\tilde{M}\rvert 3d_{z^2} d\tau$	.1481	.0000	.0000
$\int 3p_y \lvert\tilde{M}\rvert 3d_{yz} d\tau$	.0000	.0000	.2566
$\int 3p_y \lvert\tilde{M}\rvert 3d_{xy} d\tau$	.2566	.0000	.0000
$\int 3p_z \lvert\tilde{M}\rvert 3d_{x^2-y^2} d\tau$	.0000	.0000	.0000
$\int 3p_z \lvert\tilde{M}\rvert 3d_{xz} d\tau$	.0000	.2566	.0000
$\int 3p_z \lvert\tilde{M}\rvert 3d_{z^2} d\tau$	.0000	.0000	.2963
$\int 3p_z \lvert\tilde{M}\rvert 3d_{yz} d\tau$	.2566	.0000	.0000
$\int 3p_z \lvert\tilde{M}\rvert 3d_{xy} d\tau$	.0000	.0000	.0000

$$\phi_{\mu_t} = N_t r_t^{n-1} \exp(-Z_t r_t) \qquad [2.30]$$

are used in the evaluation of equation [2.28]. Thus substitution of equation [2.30] into equation [2.29], for two atomic centres t, t', gives:

$$\tilde{T} = \int N_t r_t^{n-1} \exp(-Z_t r_t) |\tilde{M}| N_{t'} r_{t'}^{n-1} \exp(-Z_{t'} r_{t'}) d\tau \qquad [2.31]$$

One-centre integrals are evaluated using spherical polar co-ordinates. For the two-centre ones, prolate spheroidal co-ordinates are used. Thus in a prolate spheroidal co-ordinate system, the atomic centres t and t' are as pictured in Fig. 2.1. Yeranos[52] refers to this type of co-ordinate system as a "re-oriented combination of co-ordinate systems". Once the two centres are placed in a re-oriented system, several useful relations can be derived between the two spherical polar systems and this re-oriented system, to facilitate the evaluation of the two centre integrals. Thus[53]:

$$\mu = \frac{r_t + r_{t'}}{R} \qquad \nu = \frac{r_t - r_{t'}}{R} \qquad \phi = \phi$$

then

$$r_t = \frac{R(\mu + \nu)}{2} \qquad r_{t'} = \frac{R(\mu - \nu)}{2}$$

$$\cos\theta_t = \frac{1 + \mu\nu}{\mu + \nu} \qquad \cos\theta_{t'} = \frac{1 + \mu\nu}{\mu - \nu}$$

$$\tilde{X} = \frac{R}{2} (\mu^2 - 1)^{1/2} (1 - \nu^2) \cos\phi \qquad [2.32]$$

$$\tilde{Y} = \frac{R}{2} (\mu^2 - 1)^{1/2} (1 - \nu^2) \sin\phi$$

$$\tilde{Z} = \frac{R}{2} (1 + \nu\mu)$$

The volume element for the integration of the prolate spheroidal co-ordinate is given by:

FIG. 2.1

Reoriented Combination
of
Co-ordinate Systems

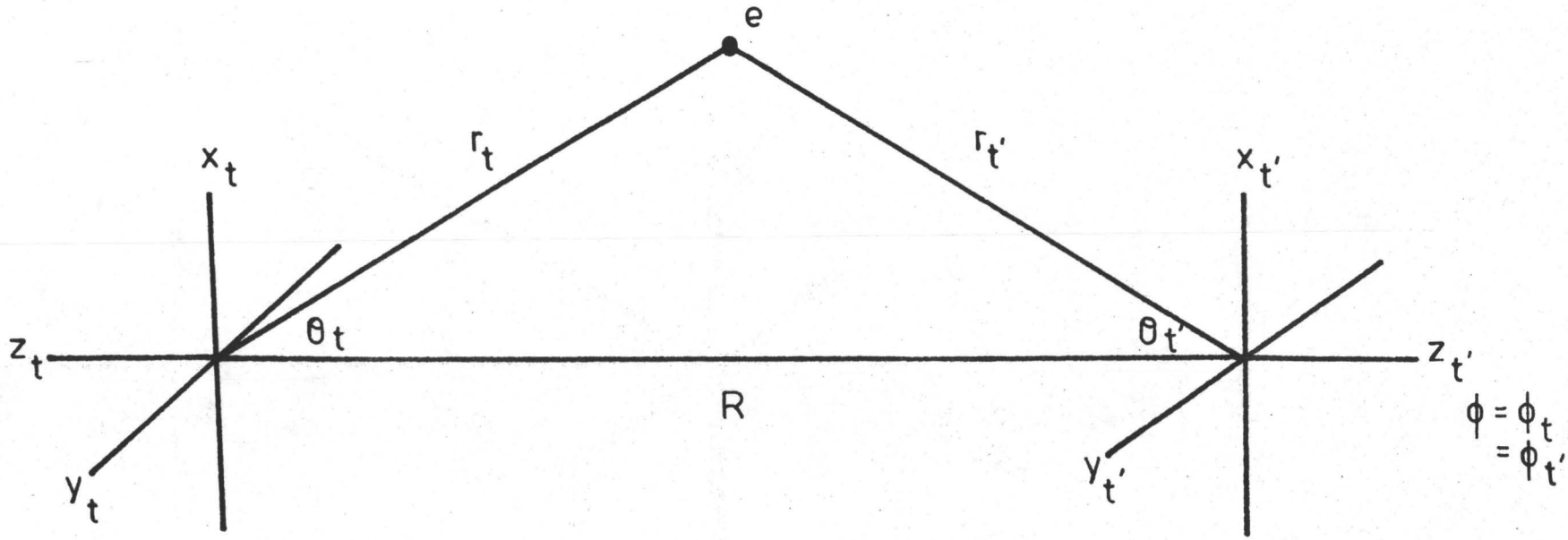

$$d\tau = \frac{R^3}{8}(\mu^2 - \nu^2)d\mu d\nu d\phi \qquad [2.33]$$

where ν: 1 to ∞

μ: -1 to +1

ϕ: 0 to 2π

Introduction of these relations into equation [2.31] yields:

$$\tilde{T} = \int_{\nu=1}^{\infty}\int_{\mu=-1}^{+1}\int_{\phi=0}^{2\pi} N_t(\tfrac{\mu+\nu}{2})\exp[-Z_t R(\tfrac{\mu+\nu}{2})]\,|\tilde{M}|\,N_{t'}\tfrac{R}{2}(\mu-\nu)\exp[-Z_{t'}R(\tfrac{\mu-\nu}{2})]\tfrac{R^3}{8}(\mu^2-\nu^2)d\nu d\mu d\phi$$

$$= \frac{N_t N_{t'}}{32}R^s\iiint(\mu+\nu)\exp[-Z_t R(\tfrac{\mu+\nu}{2})]\,|\tilde{M}|\,(\mu-\nu)\exp[-Z_{t'}R(\tfrac{\mu-\nu}{2})](\mu^2-\nu^2)d\nu d\mu d\phi \qquad [2.34]$$

In order to evaluate equation [2.32] for any value of R, N_t, $N_{t'}$, Z_t, or $Z_{t'}$, two auxiliary functions, A and B[53], are introduced:

$$A(\rho) = \int_{X=1}^{\infty} X^k\exp(-\rho x)dx = \exp(-\rho)\sum_{\mu=1}^{k+1}\frac{k!}{\rho^{\mu}(k-+1)!} \qquad [2.35]$$

$$B(\rho) = \int_{X=-1}^{+1} X^k\exp(-\rho x)dx = -\exp(-\rho)\sum_{\mu=1}^{k+1}\frac{k!}{\rho^{\mu}(k-+1)!}$$

$$-\exp(\rho)\sum_{\mu=1}^{k+1}\frac{(-1)^{k-\mu}\,k!}{\rho^{\mu}(k-+1)!} \qquad [2.36]$$

Once the two-centre expressions have been reduced to the form of integral [2.34], any two-centre problem can be expressed in terms of the integrated expressions ([2.35], [2.36]) involving the variables R, N_t, $N_{t'}$, Z_t and $Z_{t'}$.

Assumptions that were made in the one-centre calculations no longer hold for two-centre integrals. In the evaluation of $\int\phi_{2s_t}|\tilde{M}|\phi_{2p_{x_{t'}}}d\tau$ where now the 2s and $2p_x$ are on different atoms, separated by a distance R, there is a difference between (say):

$$\text{and} \quad \begin{matrix}\int\phi_{2s_C}|\tilde{M}|\phi_{2p_{x_0}}d\tau \\ \int\phi 2s_0|\tilde{M}|\phi 2p_{x_C}d\tau\end{matrix} \qquad [2.37]$$

That is, the interaction of a $2p_x$ orbital of oxygen with a 2s orbital of carbon is not the same as the interaction of a $2p_x$ orbital of carbon with a 2s orbital of oxygen. Also, from Fig. 2.1, the results of the calculation should differ according to the magnitude of r_t and $r_{t'}$. Thus a calculation done with $r_t = 0$, that is, with the electron on atomic centre t, is different from a calculation done with $r_{t'} = 0$. Both of these cases are different from the case where $r_t = r_{t'}$. Whereas in the one-centre calculation, only one integral is evaluated, in the two-centre case, it is necessary to evaluate three integrals. Since the system (of two atomic centres) does not have spherical symmetry, the p_x, p_y and p_z orbitals are no longer equivalent. If the z axis is the axis of the CO bond (say), an electron in a 2s orbital on oxygen will interact differently with the $2p_z$ orbital on carbon than with the $2p_x$ and $2p_y$ orbitals on carbon. The resulting values for the various integrals are given in Table 2.6 where the two centre integrals have been calculated for the carbonyl group in H_2CO. The values in Table 2.6 were obtained from a program written by W. A. Yeranos and made available through the Quantum Chemistry Program Exchange.

Oscillator Strength Calculations

Expressions were obtained for the moment integrals by the co-ordinate dependent method and by evaluation of the one- and two-centre integrals. A computer program was written called FCALC for this purpose.

The input for FCALC consisted of three identity cards (IDENT); an option card used to distinguish between differently ordered eigen vector matrices (IOP); the number of hydrogen nuclei, first and second row element nuclei in the molecule (LH, L1, L2); the number of atomic orbitals in each molecular orbital (N); the number of doubly occupied molecular orbitals (NOCC); the out-of-plane angle (THETA); a number distinguishing each atom (ATOM); the

x, y, and z co-ordinate of each atom (XC, YC, ZC); the atomic number of each atom (NAT); the nearest neighbours to each atom (NEIGH); and the eigen vector matrix for the molecule (C). For the molecule H_2CO the CNDO-JD program was used to generate the C matrix. For the molecules F_2CO, $C\ell_2CO$, H_2CS, F_2CS and $C\ell_2CS$ the CNDO-PD program was used.

The FCALC program is capable of calculating oscillator strengths at the three levels of approximation for molecules containing four atoms, of which up to three can be second row elements. Thus a set of thirty-one molecular orbitals can be handled.

In the output, the oscillator strengths (more exactly, the oscillator strength/transition energy) for transitions from all filled molecular orbitals to all unfilled molecular orbitals was calculated. Table 2.7 and Table 2.8 contain a comparison of the oscillator strengths obtained for formaldehyde at the three levels of approximation. Because f depends on both the transition moment and the energy of the transition, two possible f values could be calculated. One was a theoretical one, f_t (in the limits of CNDO-JD) in which the electronic transition energy E_t was obtained from a CNDO program using the expression[48]:

$$E_{ijt} = \varepsilon_i - \varepsilon_j - J_{ij} + 2k_{ij} \qquad [2.38]$$

where ε_i, ε_j are the energies of the i^{th} and j^{th} molecular orbitals;

J_{ij} is the coulomb term; and

k_{ij} is the exchange term.

NOTE: Equation [2.38] applies only to singlet-singlet transitions.

A second type of oscillator strength was a semi-empirical value f_s, in which the known transition energy E_{exp} (that is values taken from Table 2.1) was used in conjunction with the calculated transition moment. In the

Table 2.6

Two-Centre Integrals for Carbon and Oxygen

R_{CO} = 1.21 Å

	Component $\tilde{x}$ (eÅ)	$\tilde{y}$ (eÅ)	$\tilde{z}$ (eÅ)
Electron on Carbon			
$\int 2s_0 \lvert M \rvert 2p_{x_C} d\tau$	.0000	.0093	.0000
$\int 2s_0 \lvert M \rvert 2p_{y_C} d\tau$	.0093	.0000	.0000
$\int 2s_0 \lvert M \rvert 2p_{z_C} d\tau$	.0000	.0000	.0434
Electron on Carbon			
$\int 2s_C \lvert M \rvert 2p_{x_0} d\tau$	.0000	.0134	.0000
$\int 2s_C \lvert M \rvert 2p_{y_0} d\tau$	.0134	.0000	.0000
$\int 2s_C \lvert M \rvert 2p_{z_0} d\tau$	.0000	.0000	.0474
Electron on Oxygen			
$\int 2s_0 \lvert M \rvert 2p_{x_C} d\tau$	.0000	.0093	.0000
$\int 2s_0 \lvert M \rvert 2p_{y_C} d\tau$	.0093	.0000	.0000
$\int 2s_0 \lvert M \rvert 2p_{z_C} d\tau$	.0000	.0000	.0984
Electron on Oxygen			
$\int 2s_C \lvert M \rvert 2p_{x_0} d\tau$	.0000	.0134	.0000
$\int 2s_C \lvert M \rvert 2p_{y_0} d\tau$	.0134	.0000	.0000
$\int 2s_C \lvert M \rvert 2p_{z_0} d\tau$	.0000	.0000	.0573
Electron at Midpoint			
$\int 2s \lvert M \rvert 2p_x d\tau$	.0000	.0134	.0000
$\int 2s \lvert M \rvert 2p_y d\tau$	.0134	.0000	.0000
$\int 2s \lvert M \rvert 2p_z d\tau$	.0000	.0000	.0050
Electron at Midpoint			
$\int 2s \lvert M \rvert 2p_x d\tau$	.0000	.0093	.0000
$\int 2s \lvert M \rvert 2p_y d\tau$	.0093	.0000	.0000
$\int 2s \lvert M \rvert 2p_z d\tau$	.0000	.0000	.0275

Table 2.7

Comparison of Calculated Oscillator Strength Values for H_2CO

Co-ordinate Dependent Method

	$^1A_2 \leftarrow {}^1A_1(n \rightarrow \pi^*)$	$^1A_1 \leftarrow {}^1A_1(\pi \rightarrow \pi^*)$	$^1B_2 \leftarrow {}^1A_1(n \rightarrow \sigma^*)$	$^1B_1 \leftarrow {}^1A_1(\sigma \rightarrow \pi^*)$
E_{exp} (cm^{-1})	28188.	64270.	57180.	-
f_s	.0000	.2421	.0599	-
E_t (cm^{-1})	25957.	88921.	74842.	67156.
f_t	.0000	.3349	.0784	.0000
$E_{t_{C.I.}}$ (cm^{-1})	25557.	88624.	74774.	67156.
$f_{t_{C.I.}}$	.0000	.3338	.0784	.0000

One-Centre Integrals Included

	$^1A_2 \leftarrow {}^1A_1(n \rightarrow \pi^*)$	$^1A_1 \leftarrow {}^1A_1(\pi \rightarrow \pi^*)$	$^1B_2 \leftarrow {}^1A_1(n \rightarrow \sigma^*)$	$^1B_1 \leftarrow {}^1A_1(\sigma \rightarrow \pi^*)$
f_s	.0000	.2421	.0185	-
f_t	.0000	.3349	.0243	.0163
$f_{t_{C.I.}}$	.0000	.3338	.0243	.0163

Table 2.8

Calculated Oscillator Strength Values for H_2CO Including Two-Centre Integrals

Electron on Carbon or Oxygen, R_{CO} = 1.21 Å

	$^1A_2 \leftarrow {}^1A_1(n \rightarrow \pi^*)$	$^1A_1 \leftarrow {}^1A_1(\pi \rightarrow \pi^*)$	$^1B_2 \leftarrow {}^1A_1(n \rightarrow \sigma^*)$	$^1B_1 \leftarrow {}^1A_1(\sigma \rightarrow \pi^*)$
f_s	.0000	.2421	.0171	-
f_t	.0000	.3349	.0233	.0156
$f_{t_{C.I.}}$	.0000	.3338	.0233	.0156

Electron at Midpoint of Bond, R_{CO} = 1.21 Å

	$^1A_2 \leftarrow {}^1A_1(n \rightarrow \pi^*)$	$^1A_1 \leftarrow {}^1A_1(\pi \rightarrow \pi^*)$	$^1B_2 \leftarrow {}^1A_1(n \rightarrow \sigma^*)$	$^1B_1 \leftarrow {}^1A_1(\sigma \rightarrow \pi^*)$
f_s	.0000	.2421	.0171	-
f_t	.0000	.3349	.0233	.0156
$f_{t_{C.I.}}$	.0000	.3338	.0233	.0156

case of H_2CO, oscillator strengths using energy before (f_t) and after ($f_{t_{C.I.}}$) configuration interaction (see Appendix A) were obtained. Two-centre f values were calculated with the electron on the atom and at the midpoint of the bond. The two centre results are given separately in Table 2.8.

The most useful comparison of calculated and experimental results can be obtained by comparing Tables 2.7 and 2.8 with Table 2.1. The $^1A_2 \leftarrow {}^1A_1(n \rightarrow \pi^*)$ transition is formally forbidden. This fact results in an oscillator strength of zero in the three levels of approximation. Experimentally, the $^1A_2 \leftarrow {}^1A_1(n \rightarrow \pi^*)$ transition has been observed with a non-zero intensity. In order to calculate a non-zero value for the $^1A_2 \leftarrow {}^1A_1(n \rightarrow \pi^*)$ oscillator strength, theory beyond that developed to this point must be used (see Chapter 3).

The values calculated for the oscillator strength of the presumed $^1A_1 \leftarrow {}^1A_1(\pi \rightarrow \pi^*)$ transition (in all levels of approximation) fall within the limits of the empirical value quoted by King[34]. The calculated values do show the expected dependence on the transition energy. It is not possible to state which level of approximation agrees best with the experimental value, due to the uncertainty of the measured value. It should be noted that the co-ordinate dependent method and the inclusion of one-centre integrals lead to the same oscillator strength value. Also, when two-centre integrals are included, there is no change in the values. This later fact is due to the nature of the π and π^* molecular orbitals. Both are composed of 2p orbitals on carbon and oxygen. By reference to Table 2.6, it can be seen that there are no two-centre integrals between two p orbitals.

For the $^1B_2 \leftarrow {}^1A_1(n \rightarrow \sigma^*)$ calculations, the inclusion of the one-centre integrals gives results which agree most closely with the experimental value. The one-centre integral calculation using the experimental transition energy predicts a much lower f value than is observed. Since use of the CNDO-JD

transition energy (before and after configuration interaction) improves the calculated f value, the validity of the one-centre transition moment may be questioned. The two-centre calculations, using the experimental transition energy, agree closest with the experimental result. Since the σ^* molecular orbital contains 2s and 2p atomic orbitals, the contribution of the two-centre integrals will be non-zero. There is no difference, however, between the two types of two-centre calculations.

The $^1B_1 \leftarrow {}^1A_1(\sigma \rightarrow \pi^*)$ calculations show a marked difference between the co-ordinate dependent calculations and the methods including the evaluated integrals. The co-ordinate dependent method would lead one to conclude that the transition is forbidden. The one- and two-centre calculations predict that the oscillator strength should be smaller than that calculated for the $^1B_2 \leftarrow {}^1A_1(n \rightarrow \sigma^*)$ transition. The calculations including two-centre integrals do not differ significantly from the one-centre calculations. As in the $^1B_2 \leftarrow {}^1A_1(n \rightarrow \sigma^*)$ calculations, the two-centre contributions to the $^1B_1 \leftarrow {}^1A_1(\sigma \rightarrow \pi^*)$ transition lead to the same value when both types of two-centre integrals are used.

Two conclusions can be reached after examining the four transitions on which calculations for H_2CO were performed. In all cases the calculations carried out with the CNDO transition energies after configuration interaction did not differ significantly from the values obtained using CNDO-JD transition energies without configuration interaction. Also, in the three non-zero cases, inclusion of the two-centre integrals did not improve the calculated f values.

In light of the results obtained for H_2CO, calculations were carried out on F_2CO, $C\ell_2CO$, H_2CS, F_2CS, and $C\ell_2CS$, using the co-ordinate dependent method, and the inclusion of one-centre integrals only. Both the experimental transition energy (where possible) and the CNDO energy (without configuration

interaction) were used. The calculated oscillator strengths for the carbonyls are listed in Table 2.9. Table 2.10 lists the values for the thiocarbonyls. f_s denotes an oscillator strength calculated using the experimentally determined transition energy (E_{exp}) and one-centre integrals; f_t is an oscillator strength calculated using the CNDO transition energy (E_t) and the co-ordinate dependent transition moment; $f_{t_{O.C.}}$ is the oscillator strength calculated using the CNDO transition energy and the one-centre moment integrals.

The oscillator strength is a function of the transition energy. Therefore a comparison of experimental and calculated transition energies should be made before the calculated and measured f values are compared. In the eleven cases where a comparison can be made, six transition energies were calculated to be lower in energy than is observed experimentally (that is, the values quoted in Tables 2.1, 2.2). For these six, the difference between the two values ranges between 8% (for $^1A_2 \leftarrow {}^1A_1(n \rightarrow \pi^*)$ of F_2CS) and 51% ($^1A_1 \leftarrow {}^1A_1$ $(\pi \rightarrow \pi^*)$ of F_2CS). The five transitions that were calculated to be greater than found experimentally were between 31% ($^1B_2 \leftarrow {}^1A_1(n \rightarrow \sigma^*)$ in H_2CO) and 50% ($^1A_2 \leftarrow {}^1A_1(n \rightarrow \pi^*)$ in F_2CO).

Comparison of calculated oscillator strengths with the experimental values is hampered by the lack of experimental data. For H_2CO, F_2CO, $C\ell_2CO$, F_2CS and $C\ell_2CS$, the $^1A_2 \leftarrow {}^1A_1(n \rightarrow \pi^*)$ transition has been observed. Since all the compounds studied possess C_{2v} symmetry in the ground state, the $^1A_2 \leftarrow {}^1A_1$ $(n \rightarrow \pi^*)$ transition is formally forbidden, and both the one centre method and the co-ordinate dependent method predict a zero value for the oscillator strength. In the calculation of the transition energies, there is a qualitative agreement between the carbonyls and thiocarbonyls. The CNDO method predicts that the dihydrides have the lowest $^1A_2 \leftarrow {}^1A_1(n \rightarrow \pi^*)$ transition energy, the dichlorides the next lowest energy, and the difluorides the highest

Table 2.9

Calculated Oscillator Strengths for Some Carbonyls

H_2CO

	$^1A_2 \leftarrow {}^1A_1 (n \rightarrow \pi^*)$	$^1A_1 \leftarrow {}^1A_1 (\pi \rightarrow \pi^*)$	$^1B_2 \leftarrow {}^1A_1 (n \rightarrow \sigma^*)$	$^1B_1 \leftarrow {}^1A_1 (\sigma \rightarrow \pi^*)$
E_{exp} (cm^{-1})	28188.	64270.	57180.	-
f_s	.0000	.2421	.0644	-
E_t (cm^{-1})	25957.	88921.	74842.	67156.
f_t	.0000	.3349	.0784	.0000
$f_{O.C.}$	.0000	.3338	.0243	.0163

F_2CO

	$^1A_2 \leftarrow {}^1A_1 (n \rightarrow \pi^*)$	$^1A_1 \leftarrow {}^1A_1 (\pi \rightarrow \pi^*)$	$^1B_2 \leftarrow {}^1A_1 (n \rightarrow \sigma^*)$	$^1B_1 \leftarrow {}^1A_1 (\sigma \rightarrow \pi^*)$
E_{exp} (cm^{-1})	42084.	76000.	65597.	-
f_s	.0000	.0725	3.070×10^{-5}	-
E_t (cm^{-1})	62940.	68997.	96977.	93818.
f_t	.0000	.0074	.0936	.0000
$f_{O.C.}$	.0000	.0658	.0454	.0173

$C\ell_2CO$

	$^1A_2 \leftarrow {}^1A_1 (n \rightarrow \pi^*)$	$^1A_1 \leftarrow {}^1A_1 (\pi \rightarrow \pi^*)$	$^1B_2 \leftarrow {}^1A_1 (n \rightarrow \sigma^*)$	$^1B_1 \leftarrow {}^1A_1 (\sigma \rightarrow \pi^*)$
E_{exp} (cm^{-1})	33631.	-	-	-
f_s	.0000	-	-	-
E_t (cm^{-1})	47380.	62567.	79553.	50650.
f_t	.0000	.0228	.0347	.0000
$f_{O.C.}$	.0000	.0006	.0167	.0032

Table 2.10

Calculated Oscillator Strengths for Some Thiocarbonyls

H_2CS	$^1A_2 \leftarrow {}^1A_1(n \rightarrow \pi^*)$	$^1A_1 \leftarrow {}^1A_1(\pi \rightarrow \pi^*)$	$^1B_2 \leftarrow {}^1A_1(n \rightarrow \sigma^*)$	$^1B_1 \leftarrow {}^1A_1(\sigma \rightarrow \pi^*)$
E_{exp} (cm^{-1})	-	-	-	-
f_s	-	-	-	-
E_t (cm^{-1})	13409.	32107.	31646.	45823.
f_t	.0000	.1318	.0011	.0000
$f_{O.C.}$	.0000	.2122	.0012	.0528

F_2CS	$^1A_2 \leftarrow {}^1A_1(n \rightarrow \pi^*)$	$^1A_1 \leftarrow {}^1A_1(\pi \rightarrow \pi^*)$	$^1B_2 \leftarrow {}^1A_1(n \rightarrow \sigma^*)$	$^1B_1 \leftarrow {}^1A_1(\sigma \rightarrow \pi^*)$
E_{exp} (cm^{-1})	23477.1	49000.	-	-
f_s	.0000	-	-	-
E_t (cm^{-1})	21503.	24076.	28312.	41982.
f_t	.0000	.2478	4.177×10^{-4}	.0000
$f_{O.C.}$	.0000	.1218	.0028	.0368

$C\ell_2CS$	$^1A_2 \leftarrow {}^1A_1(n \rightarrow \pi^*)$	$^1A_1 \leftarrow {}^1A_1(\pi \rightarrow \pi^*)$	$^1B_2 \leftarrow {}^1A_1(n \rightarrow \sigma^*)$	$^1B_1 \leftarrow {}^1A_1(\sigma \rightarrow \pi^*)$
E_{exp} (cm^{-1})	18716.3	39793.	-	-
f_s	.0000	.1001	-	-
E_t (cm^{-1})	16329.	26883.	33774.	41455.
f_t	.0000	.1704	.0512	.0000
$f_{O.C.}$	.0000	.0677	.0149	3.814×10^{-3}

$^1A_2 \leftarrow {}^1A_1(n \rightarrow \pi^*)$ transition energy. This is also the order of electronegativity of the carbonyl (and thiocarbonyl) substituents, but any attempt to make a linear correlation fails[55]. In the carbonyls, the transition energies calculated for F_2CO and $C\ell_2CO$ are greater than the experimental values, while in the thiocarbonyls the energies for F_2CS and $C\ell_2CS$ are lower than found experimentally. In all cases the $^1A_2 \leftarrow {}^1A_1(n \rightarrow \pi^*)$ transition energy was the lowest of the four calculated transition energies. A difference is evident between the carbonyls and thiocarbonyls in both the experimental and calculated transition energies. Without exception, the carbonyl $^1A_2 \leftarrow {}^1A_1(n \rightarrow \pi^*)$ transitions are higher in energy than the corresponding thiocarbonyl compounds.

In the compounds considered, the $^1A_1 \leftarrow {}^1A_1(\pi \rightarrow \pi^*)$ transition is calculated to be the most intense transition, except in $C\ell_2CO$. Good agreement is found in H_2CO, while in F_2CO and $C\ell_2CS$, where comparison can also be made, the one-centre calculations give closer results to the experimental values than does the co-ordinate dependent method. Qualitatively the dihydrides are predicted to have the greatest intensity, followed by the difluorides and the dichlorides. The values for $C\ell_2CO$ are not consistent with the rest of the thiocarbonyls. This is due to the peculiar nature of the π molecular orbital. The contribution of the carbon 2p atomic orbital is very much less than that of the oxygen 2p. Also significant is the large contribution to the chlorine 3p's to the molecular orbital. As was the case with the $^1A_2 \leftarrow {}^1A_1(n \rightarrow \pi^*)$ transition, the transition energies for the $^1A_1 \leftarrow {}^1A_1(\pi \rightarrow \pi^*)$ transitions in the thiocarbonyls are calculated and found experimentally (for F_2CO and F_2CS) to be lower in energy than the corresponding carbonyl compounds.

The calculations for the $^1B_2 \leftarrow {}^1A_1(n \rightarrow \sigma^*)$ transitions indicate that the transition will be weaker than the $^1A_1 \leftarrow {}^1A_1(\pi \rightarrow \pi^*)$ transition, except in

$C\ell_2CO$. In H_2CS and F_2CS it is the weakest of the four transitions studied. On comparing the calculated values to the experimental data, one finds that the values for the co-ordinate dependent method, and for the inclusion of one-centre integrals, straddle the experimental values. Differences in the case of F_2CO can be attributed to the transition energy, which is calculated to be 48% larger than the experimental value. It is apparent in the thiocarbonyls that there is little effect on the transition energy when the substituents are changed from hydrogen to fluorine to chlorine. Again, all the thiocarbonyl compounds are calculated to have lower transition energies than the corresponding carbonyls.

In the $^1B_1 \leftarrow {}^1A_1(\sigma \rightarrow \pi^*)$ calculations, one sees a definite difference between the co-ordinate dependent method, and the one-centre integral method for all the compounds studied. Whereas the co-ordinate dependent method predicts a zero value for the oscillator strength, the one-centre integral method predicts a very weak transition. Except for H_2CS and F_2CS, it is predicted to be the weakest of the four transitions studied. Perhaps for this reason, the $^1B_1 \leftarrow {}^1A_1(\sigma \rightarrow \pi^*)$ transition has never been observed. Qualitatively in the thiocarbonyls the dihydrides are predicted to have the most intense $^1B_1 \leftarrow {}^1A_1(\sigma \rightarrow \pi^*)$ transitions, the fluorides the next most intense, and the chlorides the weakest. This trend is not evident in the carbonyls, but this may be a result of the energy calculations. It is significant that again all the thiocarbonyl compounds have lower calculated $^1B_1 \leftarrow {}^1A_1(\sigma \rightarrow \pi^*)$ transition energies than the corresponding carbonyl compounds. Also a very small substituent effect in the thiocarbonyls, similar to that found for the $^1B_2 \leftarrow {}^1A_1(n \rightarrow \sigma^*)$ transitions, is predicted.

Having made these comparisons using Table 2.9 and Table 2.10, it is possible to come to some general conclusions about the transitions in the

carbonyl and thiocarbonyl compounds studied.

(i) The intensities of the symmetry forbidden $^1A_2 \leftarrow {}^1A_1(n \rightarrow \pi^*)$ transitions of the carbonyls and thiocarbonyls cannot be predicted by either the co-ordinate dependent method, or by the inclusion of one-centre integrals, or, in the case of H_2CO, by the inclusion of two-centre integrals.

(ii) The two methods of calculation give similar oscillator strengths for the $^1A_1 \leftarrow {}^1A_1(\pi \rightarrow \pi^*)$ transition, except in chlorine-containing compounds. In the $^1B_1 \leftarrow {}^1A_1(\sigma \rightarrow \pi^*)$ transition, the differences between the two calculated values can be attributed to differences in the σ^* molecular orbital. The co-ordinate dependent method predicts a zero value for the oscillator strength of the $^1B_1 \leftarrow {}^1A_1(\sigma \rightarrow \pi^*)$ transition of all the compounds studied, while the one-centre method predicted a relatively weak $^1B_1 \leftarrow {}^1A_1(\sigma \rightarrow \pi^*)$ transition.

(iii) Agreement with the experimental data was good for the transitions of H_2CO. In $C\ell_2CS$ the $^1A_1 \leftarrow {}^1A_1(\pi \rightarrow \pi^*)$ values lay between the values obtained in the gas and liquid phase. In F_2CO agreement was to within a factor of three. In all cases, the calculated oscillator strengths were improved by using the experimental transition energies.

(iv) Qualitative trends could be predicted in the $^1A_1 \leftarrow {}^1A_1(\pi \rightarrow \pi^*)$ transition and the $^1B_1 \leftarrow {}^1A_1(\sigma \rightarrow \pi^*)$ transition, with respect to the intensity of the transition and the substituents. Except in $C\ell_2CO$, the $^1A_1 \leftarrow {}^1A_1(\pi \rightarrow \pi^*)$ transition is predicted to be the most intense transition of the compounds studied. In all but two cases, the $^1B_1 \leftarrow {}^1A_1(\sigma \rightarrow \pi^*)$ transitions were calculated to have the smallest oscillator strengths. In the $^1A_2 \leftarrow {}^1A_1(n \rightarrow \pi^*)$ calculations there was a qualitative agreement in the transition energies of the carbonyls and thiocarbonyls. The most significant trend throughout the calculations showed

that in all cases the carbonyl compounds were always predicted to have higher transition energies than the corresponding thiocarbonyl compounds. This trend is also evident in the experimental results, where comparison could be made.

(v) There was no apparent quantitative substituent effect in the calculated oscillator strength values. That is, the f value did not vary significantly when the different substituents were considered. The same thing was also found in the energy calculations for the $^1B_1 \leftarrow {}^1A_1(\sigma \rightarrow \pi^*)$ and $^1B_2 \leftarrow {}^1A_1(n \rightarrow \sigma^*)$ transitions of the thiocarbonyls.

The calculations on $C\ell_2CS$ were of particular interest to this work. From Table 2.10 it can be seen that three transitions, $^1A_1 \leftarrow {}^1A_1(\pi \rightarrow \pi^*)$, $^1B_1 \leftarrow {}^1A_1(\sigma \rightarrow \pi^*)$ and $^1B_2 \leftarrow {}^1A_1(n \rightarrow \sigma^*)$, are predicted to lie close together, especially since the calculated energies could carry an error of up to 25%. In practice then, the order of transition energies may be different from the calculated pattern. The transition energies may not help in the separate identification of these three transitions, but the oscillator strength calculations may. A transition similar in intensity to the $^1A_1 \leftarrow {}^1A_1(\pi \rightarrow \pi^*)$ transition could be $^1B_2 \leftarrow {}^1A_1(n \rightarrow \sigma^*)$. A transition that is much weaker than the $^1A_1 \leftarrow {}^1A_1(\pi \rightarrow \pi^*)$ transition would more likely be the $^1B_1 \leftarrow {}^1A_1(\sigma \rightarrow \pi^*)$ transition.

CHAPTER 3

THE FORBIDDEN $^1A_2 \leftarrow {}^1A_1$ TRANSITION

Introduction

The $^{1,3}A_2 \leftarrow {}^1A_1(n \rightarrow \pi^*)$ transitions in the carbonyl and thiocarbonyl groups of X_2CO (or X_2CS) type molecules are formally forbidden when the molecules possess C_{2v} symmetry. However, absorption transitions to the $^1A_2(\pi^*,n)$ state have been observed in H_2CO[36], F_2CO[42], Cl_2CO[43], F_2CS[44] and Cl_2CS[33], while that to the $^3A_2(\pi^*,n)$ state has been observed in H_2CO[36,37], F_2CS[45], and Cl_2CS[47]. Simple oscillator strength calculations (of the type carried out in Chapter 2) cannot account for the intensity of these transitions.

Two methods have been used in this chapter to calculate the intensity of the $^1A_2 \leftarrow {}^1A_1(n \rightarrow \pi^*)$ transition in H_2CO and Cl_2CS. The first is developed by expanding the oscillator strength in a Taylor's series. The second is a vibrational-electronic interaction method.

The vibrational-electronic interaction method was first used by Pople and Sidman[60] in a study of the oscillator strength of the $^1A_2 \leftarrow {}^1A_1$ transition in H_2CO. The calculations presented here were undertaken for two reasons. Firstly, Pople and Sidman used a simple LCAO method to construct molecular orbitals used in the calculation. It was felt by this investigator that it would be of interest to see what improvement (if any) would result from using molecular orbitals obtained from a CNDO program. Secondly the vibrational-electronic interaction method is a semi-empirical calculation. The calculations carried out here make use of experimental data that was not available to Pople and Sidman.

Expansion of the Oscillator Strength

It was found that for the planar configuration, the three carbonyls and three thiocarbonyls studied were predicted to have zero oscillator strengths.

If the molecules become bent, they can be assigned to the C_s point group, and the $^1A_2 \leftarrow {}^1A_1(n \rightarrow \pi^*)$ transition is no longer forbidden. Calculations of the type described in Chapter 2 were carried out on H_2CO and $C\ell_2CS$ (the CNDO-JD program was used for H_2CO, while the CNDO-PD program was used for $C\ell_2CS$), for various bent geometries. The results of these calculations are given in Table 3.1.

The oscillator strength is a function that can be expanded in a Taylor's series with respect to the variable Q (in this case the internal co-ordinate corresponding most closely to the bending of the carbon-oxygen bond out of the plane formed by the carbon and two hydrogens, in H_2CO)[74,75]. Thus:

$$f_Q = f_o + \left(\frac{\partial f}{\partial Q}\right)_o Q + \frac{1}{2}\left(\frac{\partial^2 f}{\partial Q^2}\right)_o Q^2 + \ldots\ldots \qquad [3.1]$$

where the subscript o implies that the evaluation is carried out at the equilibrium position.

In equation [3.1], f_o is zero for an $^1A_2 \leftarrow {}^1A_1$ transition of a planar C_{2v} molecule, and so can be neglected from further considerations. Since f is proportional to the square of $\tilde{R}$, it is an even function of Q, and therefore has a minimum at Q = 0, so the derivative of the linear term is zero. Equation [3.1] thus reduces to:

$$f_Q = \frac{1}{2}\left(\frac{\partial^2 f}{\partial Q^2}\right)_o Q^2 \qquad [3.2]$$

The oscillator strength can be calculated for various bent configurations. f can thus be expressed as a function of θ, the out-of-plane angle. The relation between f and θ can be given as:

$$f_\theta = \frac{1}{2}\left(\frac{\partial^2 f}{\partial \theta^2}\right)_o \theta^2 \qquad [3.3]$$

What is needed is a relation between equation [3.2] and equation [3.3].

$$\text{If} \quad \frac{\partial^2 f}{\partial Q^2} = \frac{\partial^2 f}{\partial \theta^2}\frac{\partial \theta^2}{\partial Q^2} = \frac{\partial^2 f}{\partial \theta^2}\left(\frac{\partial \theta}{\partial Q}\right)^2 \qquad [3.4]$$

and[57]:

$$\theta = QG^{1/2} \qquad [3.5]$$

where G is the G matrix element.

Then

$$\frac{\partial \theta}{\partial Q} = G^{1/2} \qquad [3.6]$$

Substitution of relation [3.6] into equation [3.4] gives:

$$\frac{\partial^2 f}{\partial Q^2} = \left(\frac{\partial^2 f}{\partial \theta^2}\right)_o G \qquad [3.7]$$

The relation in equation [3.3] can be rearranged to:

$$\left(\frac{\partial^2 f}{\partial \theta^2}\right)_o = \frac{2f_\theta}{\theta^2} \qquad [3.8]$$

Equation [3.2] can thus be rewritten as:

$$f_Q = \frac{1}{2}\left(\frac{\partial^2 f}{\partial Q^2}\right)_o Q^2 = \frac{1}{2}\left(\frac{\partial^2 f}{\partial \theta^2}\right)_o Q^2 G \qquad [3.9]$$

Q can be calculated from the relation:

$$\bar{Q}^2 = \frac{h}{8\pi^2 c\nu} \qquad [3.10]$$

where ν is one of the 3N-6 fundamental ground state vibrational frequencies (for these calculations, the vibration corresponding to inversion of the pyramidal molecule was used).

G can be calculated from the internal co-ordinates of the molecule[57].

In using equation [3.5] it is assumed that the ground and excited state potential energy curves are exactly similar. If they are not, centroids must be employed[34].

Ideally the calculation should be carried out for very small displace-

ments. The results listed in Table 3.1 are not constant with varying θ, as would be expected. The CNDO-JD molecular orbitals change as the geometry is varied, and these changes result in a non-constant f value. For these calculations both the combining states must be bent to the same extent.

The results for H_2CO and $C\ell_2CS$ for out-of-plane angles up to 15° are listed in Table 3.2. The results for H_2CO are less sensitive to geometry changes than those for $C\ell_2CS$. The comparison with the experimental values indicate that the calculated values are much lower than the experimental values. A possible explanation could be the fact that both combining states were considered to be bent. Experimentally, however, it has been established that the ground state is planar while the $^1A_2(\pi^*,n)$ state is bent 32° out of plane.

Vibrational Electronic Interaction

The theory developed here is essentially a review of the developments given by Pople and Sidman[60] and Murrell and Pople[74]. Results from perturbation theory will be used without proof. The development of perturbation theory can be found elsewhere. Pople-Sidman notation will be used here.

The total wave function Ψ can be written in the form:

$$\Psi_{k\ell}(X,Q) = \textcircled{H}_k(X,Q)\Phi_{k\ell}(Q) \qquad [3.13]$$

where X represents electronic co-ordinates;

Q represents nuclear co-ordinates;

ℓ is a vibrational quantum number; and

k is used to designate the electronic state.

In equation [3.13] $\textcircled{H}(X,Q)$ represents a solution of the electronic Schrödinger equation for a fixed nuclear configuration, while $\Phi_{k\ell}(Q)$ is a vibrational wave function associated with the electronic state k.

For each molecular configuration Q, the transition moment for the absorption transition $k \leftarrow 0$ is given by:

Table 3.1

Calculated Oscillator Strengths for the $^1A_2 \leftarrow {}^1A_1(n \rightarrow \pi^*)$ Transitions of H_2CO and $C\ell_2CS$

θ (out-of-plane angle)	H_2CO f_θ	$C\ell_2CS$ f_θ
0.0°	.00	.00
5.0°	5.94×10^{-5}	0.65×10^{-3}
7.5°	1.31×10^{-4}	1.00×10^{-3}
10.0°	2.28×10^{-4}	1.21×10^{-3}
15.0°	7.94×10^{-4}	1.39×10^{-3}

NOTE: The energies used in the calculations were the experimental transition energies (Tables 2.1, 2.2); only one-centre integrals were used in the calculations.

Table 3.2

Calculated Oscillator Strengths of the $^1A_2 \leftarrow {}^1A_1(n \rightarrow \pi^*)$ Transitions of H_2CO and $C\ell_2CS$ Using the Expanded Oscillator Strength Method

θ (out-of-plane angle)	H_2CO f_Q	$C\ell_2CS$ f_Q
0.0°	.00	.00
5.0°	6.88×10^{-5}	5.83×10^{-7}
7.5°	6.72×10^{-5}	3.84×10^{-7}
10.0°	6.59×10^{-5}	2.69×10^{-7}
15.0°	6.20×10^{-5}	1.46×10^{-7}

NOTE: f_Q's were calculated using the experimental transition energies (Tables 2.1, 2.2).

$$M_{k\leftarrow 0}(Q) = \int \textcircled{H}_o(X,Q)\ M\textcircled{H}_k(X,Q)dX \qquad [3.14]$$

If the dipole moment operator M is referred to a cartesian set of axes rotating with the molecule, then the oscillator strength of that part of the vibronic transition $k\ell \leftarrow om$ which is polarized in the x direction (say) is given by:

$$f^{(x)}_{k\ell\leftarrow om} = \frac{8\pi^2 m_e c}{3h^2e^2} E_{k\ell\leftarrow om} \left| \int \Phi_{om}(Q) M^x_{ok}(Q) \Phi_{k\ell}(Q) dQ \right|^2 \qquad [3.15]$$

where $E_{k\ell\leftarrow om}$ is the energy of the transition.

The total intensity of the part of the electronic transition which is x polarized is given by:

$$f^{(x)}_{k\leftarrow o} = \sum_{\ell} f^{(x)}_{k\ell\leftarrow oo} \qquad [3.16]$$

If only the sum over ℓ is desired $E_{k\ell\leftarrow oo}$ can be replaced by an average $E_{k\leftarrow o}$. The functions $\Phi_{k\ell}(Q)$ form a complete set (in the vibrational co-ordinates). Application of the quantum mechanical sum rule[59] gives:

$$f^{(x)}_{k\leftarrow o} = \frac{8\pi^2 m_e c}{3h^2e^2} E_{k\leftarrow o} \langle (M^x_{ok})^2 \rangle_{av} \qquad [3.17]$$

where $\langle (M_{ok})^2 \rangle_{av}$ is the mean square of the transition moment.

The total oscillator strength is the sum of the x, y and z polarized oscillator strengths.

The mean square transition moment is calculated by finding the extent to which the electronic function $\textcircled{H}_k(X,0)$ is mixed with the wave function of another excited state $\textcircled{H}_s(X,0)$ by nuclear vibration[74]. If the transition $s \leftarrow o$ is allowed, then there can be intensity borrowing by the transition $k \leftarrow o$ (in these calculations $^1A_2 \leftarrow {}^1A_1$). The ratio of the oscillator strengths of the two transitions is given by perturbation theory as:

$$\frac{f_{k\leftarrow o}}{f_{s\leftarrow o}} = \left(\frac{W_{ks}}{E_{k\leftarrow o} - E_{s\leftarrow o}}\right)^2 \frac{E_{k\leftarrow o}}{E_{s\leftarrow o}} \qquad [3.18]$$

where W_{ks} is the vibrational-electronic interaction energy matrix element between the excited electronic states k and s; and

$E_{k\leftarrow o}$, $E_{s\leftarrow o}$ are the transition energies for the transitions from the o (ground) to the k and s states respectively.

In this study the $^1B_1 \leftarrow {}^1A_1(n \rightarrow \sigma^*)$ and $^1B_2 \leftarrow {}^1A_1(\sigma \rightarrow \pi^*)$ transitions were the allowed transitions lending intensity to the $^1A_2 \leftarrow {}^1A_1(n \rightarrow \pi^*)$ transition.

W_{ks} is defined by:

$$W_{ks} = \int \psi_1(X_i) \left[\sum_{\sigma}^{\text{all nuclei}} Z_\sigma e^2 \left(\frac{\partial \tilde{r}}{\partial Q_a}\right)_o \frac{\tilde{r}_{i\sigma}}{r_{i\sigma}^3} (\overline{Q_a^2})^{1/2} \right] \psi_2(X_i) dX_i \qquad [3.19]$$

where ψ_1, ψ_2 are unmatched molecular orbitals in the excited electronic wave function undergoing mixing;

i labels the electrons;

σ labels the nuclei;

X_i are the electron co-ordinates;

Z_e is the nuclear charge;

Q_a is the normal co-ordinate; and

$\tilde{r}_{i\sigma}$ is the vector from electron i to nucleus σ.

$(\overline{Q_a^2})^{1/2}$ is called the root-mean square displacement in the zero vibrational state of the a^{th} normal mode (ν_a) in the ground state. The relation between $(\overline{Q_a^2})^{1/2}$ and ν_a is given by[60]:

$$(\overline{Q_a^2})^{1/2} = \frac{h}{8\pi\nu_a} \qquad [3.20]$$

Equation [3.19] represents the electrostatic energy of interaction between a set of dipoles $\tilde{\mu}$, defined by:

$$\tilde{\mu}_\sigma = Z_\sigma e \left(\frac{\partial \tilde{r}_\sigma}{\partial Q_a}\right)_o (\overline{Q_a^2})^{1/2} \qquad [3.21]$$

where the derivatives $(\frac{\partial r_\sigma}{\partial Q_a})_o$ are the elements of the matrix which transforms normal co-ordinates to cartesian displacement co-ordinates (see Appendix C);

and the electronic distribution $e\psi_1\psi_2$. $e\psi_1\psi_2$ is called the transition density (between states 1 and 2)[61].

Mixing of Excited States by Vibrations

The $^1A_2 \leftarrow {}^1A_1$ transition is formally forbidden by electronic selection rules. However, the transition may have a non-zero intensity if the $^1A_2(\pi^*,n)$ excited state is mixed (Pople-Sidman notation) with some other excited state by means of one of the normal vibrations.

For an excited state k to become "vibrationally induced"[60], the following must hold:

$$\Gamma(Q_a) = \Gamma(k) \otimes \Gamma(s)$$

where $\Gamma(k)$ is the representation to which the upper state (k) of the forbidden transition belongs;

$\Gamma(s)$ is the representation to which the upper state (s) of an allowed transition belongs; and

$\Gamma(Q_a)$ is the representation to which the normal vibration belongs.

In H_2CO, the $^1A_2(\pi^*,n)$ excited state will mix with the $^1B_2(\sigma^*,n)$ excited state (say) when a vibration Q_a is used such that:

$$\Gamma(Q_a) = A_2 \otimes B_2 = b_1$$

That is, a vibration of b_1 symmetry (i.e., ν_4 in H_2CO) can mix the two excited states. In a similar manner ν_5 and ν_6 (in H_2CO) are of b_2 symmetry and can mix the $^1A_2(\pi^*,n)$ and $^1B_1(\pi^*,\sigma)$ states.

The molecular orbitals used in the calculations were obtained from a CNDO program (the program written by Dr. D. P. Santry was used for H_2CO; the

program written by Pople and Dobosh was used for $C\ell_2CS$), and are listed in Table 3.3. The geometries listed in Table 2.3 were used in the CNDO calculations.

The results of the calculations are listed in Tables 3.4 and 3.5. The contribution of the different vibrations (ν_4, ν_5, ν_6) are separated for clarity.

The results for H_2CO are in good agreement with the experimental value of 2.4×10^{-4}. The conclusion that the $^1B_2 \leftarrow {}^1A_1(n \rightarrow \sigma^*)$ transition contributes more intensity to the $^1A_2 \leftarrow {}^1A_1(n \rightarrow \pi^*)$ transition, than the $^1B_1 \leftarrow {}^1A_1(\sigma \rightarrow \pi^*)$ transition is similar to that of Pople and Sidman. However the experimental transition energy of the $^1B_2 \leftarrow {}^1A_1(n \rightarrow \sigma^*)$ transition used in this calculation, makes the resulting oscillator strength more reliable. Compared to the calculations of Pople and Sidman, the perturbing b_2 vibrations in this calculation are more important. This is a result of the refined estimate of the $^1B_1 \leftarrow {}^1A_1(\sigma \rightarrow \pi^*)$ transition energy obtained from the CNDO calculations.

The $C\ell_2CS$ calculations are less satisfying. Again the $^1B_2 \leftarrow {}^1A_1(n \rightarrow \sigma^*)$ transition is calculated to be the main contributor of intensity to the $^1A_2 \leftarrow {}^1A_1(n \rightarrow \pi^*)$ transition. However, the intensity found experimentally is one-third of that predicted by these calculations. Intensity borrowing via the two b_2 vibrations would contribute less intensity than is found experimentally. Pople and Sidman explained the lesser importance of the $^1B_1 \leftarrow {}^1A_1(\sigma \rightarrow \pi^*)$ contribution in H_2CO as being due to the nature of the transition density. Their molecular orbitals were such that only oxygen contributed to the transition density in the $^1B_2 \leftarrow {}^1A_1$ case. This explanation, however, cannot be used when CNDO molecular orbitals are used in the calculations for H_2CO and $C\ell_2CS$.

As a result of the two calculations, the $^1A_2 \leftarrow {}^1A_1(n \rightarrow \pi^*)$ oscillator

strength has been calculated to have a non-zero value, unlike the calculations carried out in Chapter 2. Agreement with the experimental values is best for the vibration dipole interaction method; however to carry out this calculation the L matrix must be known and molecular orbitals must be obtained (for example, from a CNDO program). The expansion of the oscillator strength method predicts a lower value than is found experimentally and the method requires the setting up of a program similar to the one described in Chapter 2, as well as obtaining eigen values from a CNDO program.

Table 3.3

Molecular Orbital Coefficients Obtained from CNDO

H_2CO

	$2s_C$	$2s_O$	$2p_{x_C}$	$2p_{x_O}$	$2p_{y_C}$	$2p_{y_O}$	$2p_{z_C}$	$2p_{z_O}$
σ	.0159	-.2903	.4993	-.7635	.0000	.0000	.0000	.0000
π	.0000	.0000	.0000	.0000	.0000	.0000	.6477	.7619
n	.0000	.0000	.0000	.0000	-.2940	.7739	.0000	.0000
π^*	.0000	.0000	.0000	.0000	.0000	.0000	.7619	-.6477
σ^*	-.6142	.0617	.2469	-.1511	.0000	.0000	.0000	.0000

$C\ell_2CS$

	$2s_C$	$3s_S$	$2p_{x_C}$	$3p_{x_S}$	$2p_{y_C}$	$3p_{y_S}$	$2p_{z_C}$	$3p_{z_S}$
σ	.0324	-.1953	.3319	-.3915	.0000	.0000	.0000	.0000
π	.0000	.0000	.0000	.0000	.0000	.0000	-.3781	-.5552
n	.0000	.0000	.0000	.0000	.1881	-.8648	.0000	.0000
π^*	.0000	.0000	.0000	.0000	.0000	.0000	-.4849	.7476
σ^*	-.4809	.1347	.1791	-.3789	.0000	.0000	.0000	.0000

Table 3.4

Vibration Dipole-Transition Density Interaction

for H_2CO

Zero Point Vibration Dipole (units Å e)

Q_4	Q_5	Q_6
.1065	.0839	.1887

Transition Density

$Q_4 - Q_5$	Q_6
$n\sigma = -.0042\ 2s_C 2p_y$	$\sigma^*\pi^* = -.4680\ 2s_C 2p_y$
$-.2247\ 2s_O 2p_y$	$=.0399\ 2s_O 2p_y$

Dipole Moment - One-Centre Terms (units Å e)

$Q_4 - Q_5$	Q_6
carbon = .0016	carbon = .1637
oxygen = .0650	oxygen = .0115

Interaction Energy W (units eV)

Q_4	Q_5	Q_6
.0053	.0012	.087

Oscillator Strength of $\pi^* \leftarrow n$ Transition

f	5.45×10^{-5}	1.23×10^{-5}	4.50×10^{-4}

Table 3.5

Vibration Dipole-Transition Density Interaction

for $C\ell_2CS$

Zero Point Vibration Dipole (units Åe)

Q_4	Q_5	Q_6
9.498	9.634	9.661

Transition Density

$Q_4 - Q_5$	Q_6
$n\sigma = .0061\ 2s_C 2p_{y_C}$	$\sigma^*\pi^* = .2332\ 2s_C 2p_{z_C}$
$+.1689\ 3s_S 3p_{y_S}$	$+.1007\ 3s_S 3p_{z_S}$

Dipole Moment - One-Centre Terms (units Åe)

$Q_4 - Q_5$	Q_6
carbon = .0021	carbon = .0816
sulphur = .0493	sulphur = .0294

Interaction Energy W (units eV)

Q_4	Q_5	Q_6
.0257	.0260	.0194

Oscillator Strength of $\pi^* \leftarrow n$ Transition

1.28×10^{-6}	1.30×10^{-6}	1.01×10^{-4}

CHAPTER 4

THEORY OF ULTRA-VIOLET SPECTROSCOPY

Introduction

The remainder of this thesis will be devoted to the vibrational analysis of the $\pi^* \leftarrow \pi$ system and the interpretation of the unknown system of $C\ell_2CS$. A brief introduction to the theory of vibrational spectroscopy and the methods used in the analysis will be given first.

Vibrational Structure of an Electronic Spectrum

Consider two electronic states of a molecule with energies E', E''. In each state, the molecule has characteristic kinetic energy (T_k) and potential energy (V) functions for internal vibration. The potential energy function can be expressed algebraically, and can take either a harmonic form or an anharmonic form. This potential energy expression can be substituted into the quantum mechanical wave equation in order to solve for vibrational eigenvalues and eigenvectors. If the potential is assumed to be harmonic, the resulting eigenvalues take the form:

$$E_\nu = (v + \tfrac{1}{2})h\nu_c \qquad [4.1]$$

where $v = 0, 1, 2, ...;$

v is called the vibrational quantum number; and

ν_c is the classical vibrational frequency.

The result, then, is a set of vibrational levels separated by a constant energy $h\nu_c$. Each of the vibrational levels has a corresponding eigenfunction, which is a function of the nuclear co-ordinates. The symmetry of each level can be obtained by operating on the eigenfunction corresponding to each level by the symmetry operators of the point group to which the molecule belongs.

In many cases the potential energy cannot be assumed to be harmonic.

Then the vibrational term values can be described empirically by:

$$G_\nu = \sum_i w_i (v_i + \tfrac{1}{2}) + \sum\sum_{ij} x_i (v_i + \tfrac{1}{2})(v_j + \tfrac{1}{2}) + \ldots \qquad [4.2]$$

where v_i, v_j = 0, 1, 2, ...,

w_i, x_i are constants.

In terms of wavenumbers, all possible vibrational transitions of an electronic transition can be represented by:

$$\nu = \nu_e + G'(v_1', v_2', v_3', \ldots) - G''(v_1'', v_2'', v_3'', \ldots) \qquad [4.3]$$

where a single prime superscript denotes the upper state; and

a double prime superscript denotes the lower state;

and
$$\nu_e = T_e' - T_e'' \qquad [4.4]$$

where T_e', T_e'' are the relative energies of the potential minima (in cm^{-1}).

Double-Well Potential Function

If a molecule of the type considered here (i.e., X_2CO or X_2CS) is non-planar in a particular electronic state, it can exist in either of two different geometrical configurations. For example, the sulphur-carbon bond of $C\ell_2CS$ can be bent out of the plane containing the carbon and the two chlorines. If the molecules were fixed in space, one would be able to distinguish between configurations bent by an angle $+\theta$ or $-\theta$ that the sulphur-carbon bond makes with the $CC\ell_2$ plane (see Fig. 4.1). The two possible bent configurations each have a potential energy function that may be expressed algebraically. In harmonic oscillator approximation equation [4.1] could be used to describe the vibrational levels of each configuration. Since the two geometrical configurations are related by the operation of inversion at the centre of mass, the potential functions for the two configurations will

FIG. 4.1

Bent Configurations
of
Cl_2CS

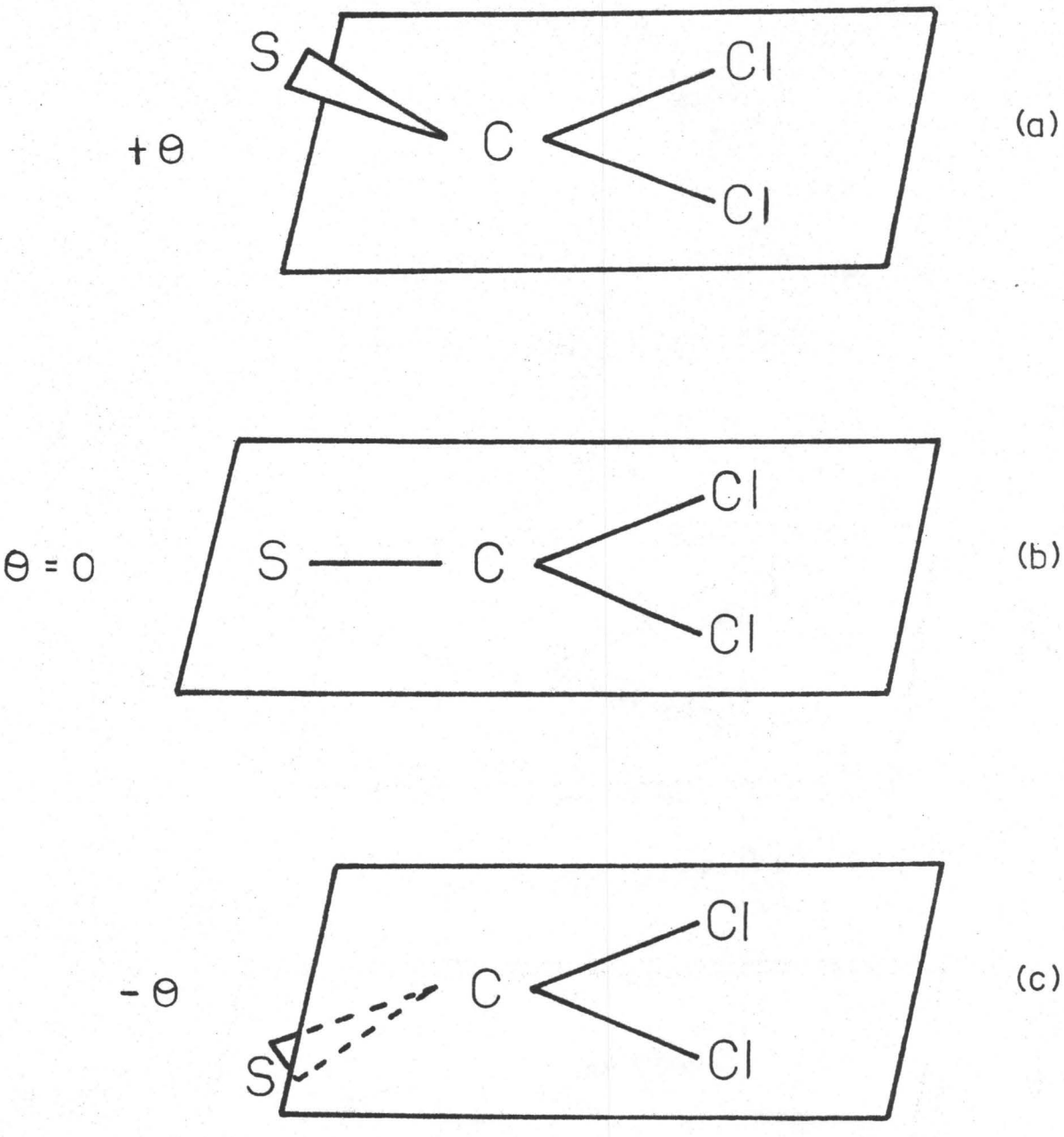

be identical. Each of the vibrational levels will be doubly degenerate.

In the strict harmonic case, the two molecular configurations will be separated by an infinitely high potential barrier (see Fig. 4.2c). This implies that the physical interconversion of the two bent configurations also requires an infinite amount of energy. If the interconversion of the two configurations is energetically possible, then the potential surface used to describe the electronic state lies between the limits of a harmonic potential surface (Fig. 4.2a) and two separate harmonic surfaces (Fig. 4.2c). The result is a potential surface that takes the form of a double well (Fig. 4.2b). In this case, the vibrational levels of the two configurations are no longer exactly degenerate, but have a splitting between the pairs of vibrational (inversion doubling) levels. (NOTE: The vibrational levels in Fig. 4.2b are labelled consecutively 0, 1, 2, 3, ..., but the alternate labelling 0^+, 0^-, 1^+, 1^-, ..., which groups the levels into split pairs may be used.) The splitting between the pairs of vibrational levels is small near the bottom of the potential wells, but increases rapidly as the levels approach the top of the potential barrier to inversion. Also, the higher the barrier to inversion, the more the pairs of vibrational levels at lower energies will behave like the levels of a harmonic oscillator, and the smaller the splitting between the pairs of vibrational levels. The splitting between pairs of the vibrational levels is called the inversion doubling splitting.

As an illustrative example, $C\ell_2CS$ will be considered. $C\ell_2CS$ is known to be planar in the ground state[73], and is known to be bent in the $^1A_2(\pi^*,n)$ state. ν_4 (see Fig. 1.1) corresponds to motion that would lead to a pyramidal configuration. Some possible vibrational transitions between the ground and excited state are shown in Fig. 4.3. It should be noted that although the excited state is assumed to be bent, the delocalized domain has C_{2v} symmetry.

FIG. 4.2
Vibrational levels for Different Heights of
Potential Barrier to Inversion

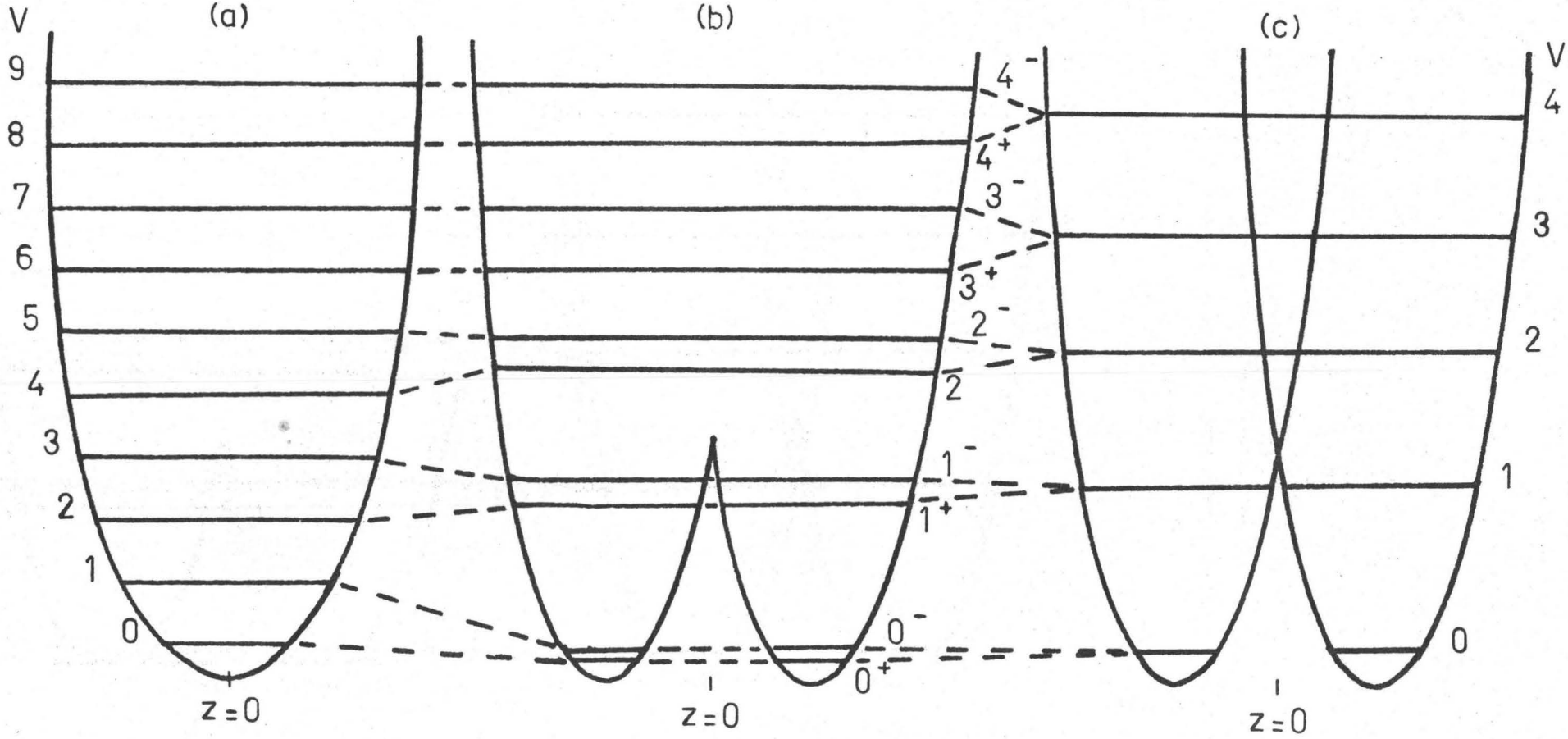

Fig. 4.3

Vibrational Transitions Between the Ground and $A_2(\pi^*,n)$ Excited State of $C\ell_2CS$

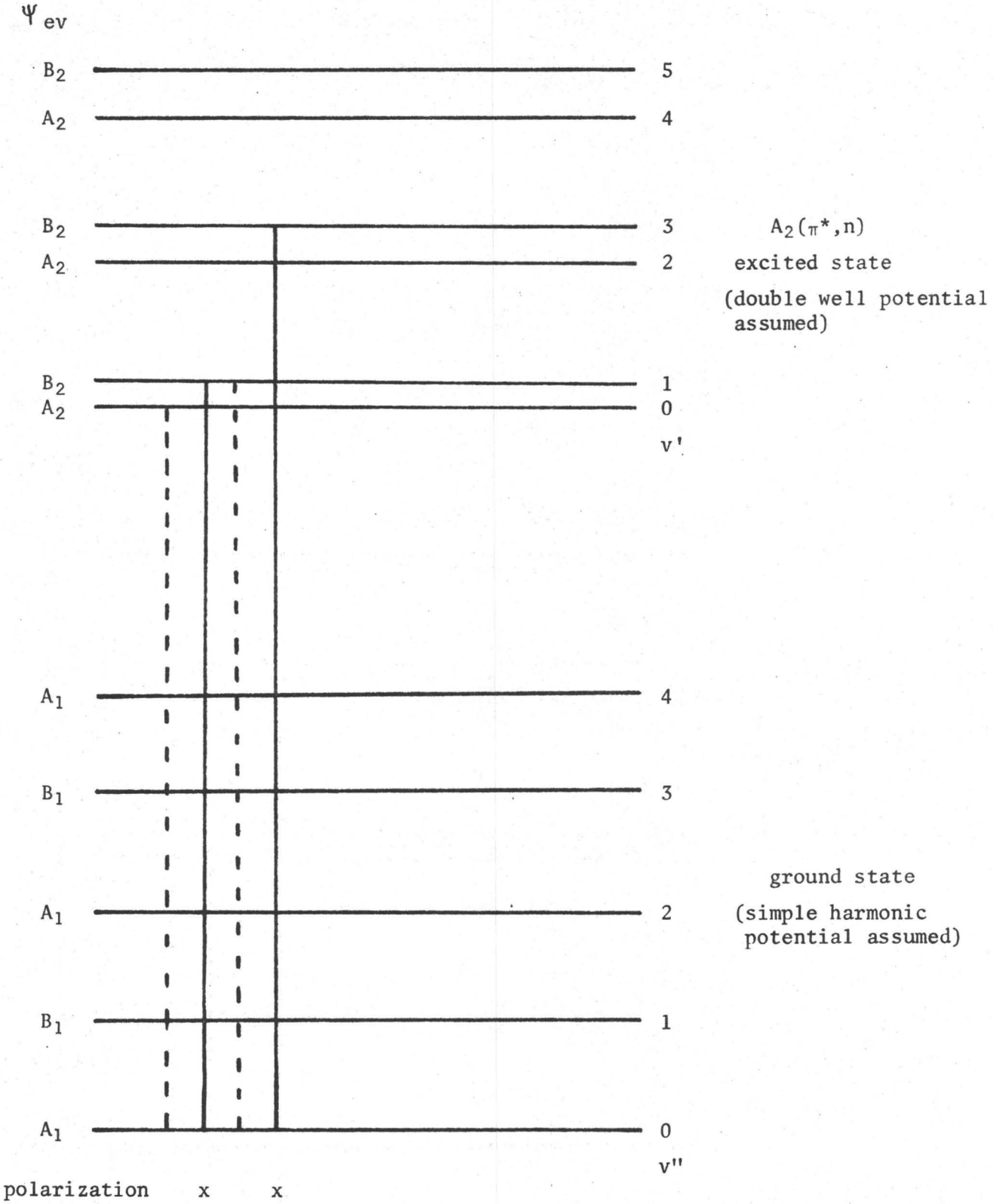

The vibrational wavefunctions are classified under this point group in both the ground and excited states of $C\ell^{35}C\ell^{35}CS$ and $C\ell^{37}C\ell^{37}CS$. Brand et al.[15] made this approximation in their study of the $^1A_2 \leftarrow {}^1A_1$ transition because the barrier to inversion was low.

The polarization of the transition is determined from the symmetry of the vibronic wave functions (see later).

Electronic and Vibrational Selection Rules[34]

The total wave function Ψ can be replaced by the vibronic (vibrational-electronic) wave function $\psi_e\psi_v$, since the stationary states for nuclear vibrational motion is independent of the angle of orientation during rotation. Then the transition moment integral can be separated into electronic and vibrational parts:

$$\tilde{R} = \int \psi'_{ev} |\tilde{M}| \psi''_{ev} d\tau = \int \psi'_e |\tilde{M}_e| \psi''_e d\tau_e \int \psi'_v \psi''_v d\tau_v \qquad [4.5]$$

The electronic transition between the two states described by ψ'_e and ψ''_e is "allowed" if the selection rule given by equation [2.19] is satisfied. The transition is x (or y or z) polarized if $\tilde{M}$ is replaced by $e\tilde{x}$ (or $e\tilde{y}$ or $e\tilde{z}$).

The integral $\int \psi'_v \psi''_v d\tau_v$ determines the relative intensities of the transitions between individual vibrational levels in the combining electronic states. In order that the integral be non-zero:

$$\Gamma(\psi'_v) \otimes \Gamma(\psi''_v) \quad \propto \quad \text{totally symmetric group representation} \qquad [4.6]$$

Equation [4.6] will be true if ψ''_v and ψ'_v belong to the same symmetry species. If the transition is electronically allowed, the vibrationaless levels ($v'_i = 0$, $v''_i = 0$, $i = 1$, number of vibrations) will always combine to give the origin transition. Also levels in which any number of quanta of totally symmetric vibration are excited in either electronic state can also combine. Non-totally symmetric vibrations can occur when $v'_i - v''_i = 0, 2, 4, \ldots$, for [4.6]

to be satisfied. If the dipole moment operator is expressed as a function of nuclear displacements, the electronic transition elements differ from zero as soon as the nuclei leave their equilibrium positions, and can cause bands for which single quantum excitation of non-totally symmetric vibrations provide false origins to appear weakly in the spectrum[54].

Combining electronic levels may be perturbed by other levels of proper symmetry, through the normal displacement (ξ). ξ makes a transition allowed if an electronic level exists that can combine with ψ_e'', and differs from ψ_e' by the transformation properties of ξ[54]. See Chapter 3, references (60, 54).

Double Minimum Potential

J. B. Coon, N. W. Naugle and R. D. McKenzie[88] constructed a three-parameter double minimum potential function by superimposing a Gaussian function and a harmonic oscillator potential function. In order to determine the potential function in terms of a mass adjusted co-ordinate (Q), three spectroscopic quantities (a level interval, an isotope shift, a band intensity ratio) must be known.

The double-minimum potential function has the form:

$$V(Q) = \frac{1}{2}\lambda Q^2 + A \exp(-a^2Q^2) \qquad [4.6]$$

The minimum of the function Q_m (really Q_m^2) is obtained by differentiation:

$$Q_m^2 = \left(\frac{1}{a^2}\right) \ln\left(\frac{2a^2A}{\lambda}\right) \qquad [4.7]$$

A parameter ρ is defined by:

$$a^2 = \frac{e^{\rho}\lambda}{2A} \qquad [4.8]$$

By increasing ρ, the outer walls of the potential function rise less steeply than the walls of the barrier.

The barrier height b (in cm^{-1}) is given by:

$$b = B\nu_o \qquad [4.9]$$

where ν_o is obtained from $\lambda = (2\pi c\nu_o)^2\rho$

B is obtained from $Bhc\nu_o = A\frac{(e^\rho - \rho - 1)}{e^\rho}$

In terms of ν_o, B and ρ, Q_m^2 becomes:

$$Q_m^2 = \left(\frac{2\rho}{e^\rho-\rho-1}\right)\frac{h}{4\pi^2 c}\frac{B}{\nu_o} \qquad [4.10]$$

Coon et al.[88] have tabulated the eigenvalues for equation [4.6] for various values of ρ, B and ν_o.

The energy levels $\left(\frac{G}{\nu_o}\right)$ are calculated relative to the potential minimum using:

$$\frac{G}{\nu_o} = \frac{E}{hc\nu_o} - \frac{B(\rho+1)}{e^\rho-\rho-1} \qquad [4.11]$$

where $\frac{E}{hc\nu_o}$ is the zero reference for the levels.

The vibrational energy (in cm^{-1}) relative to the 0^+ levels (say) is given by:

$$G(\nu_i) = G(0^+) + G_o(\nu_i) \qquad [4.12]$$

In the calculations carried out in this work, a theoretical value of the ratio $\frac{G(1^+) - G(0^+)}{G(0^-) - G(0^+)}$ was calculated and compared to the experimental ratio. The values of ρ and B were varied until the two ratios were the same. The values of ρ, B and ν_o were then used to calculate the ten lowest energy levels of the double minimum using the tables in reference (88).

The out-of-plane angle (θ) can be determined using

$$\theta = \frac{Q_m}{\mu^{1/2} r} \qquad [4.13]$$

where for H_2CO, r is the carbon-oxygen distance; and

μ is the reduced mass.

The reduced mass for formaldehyde (an analogous expression was used for

$C\ell_2CS$) is given by Coon et al. as:

$$\frac{1}{\mu} = \left(\frac{1}{M_O} + \frac{1}{M_C}\right) + \frac{2}{M_C}\frac{r}{Z} + \left(\frac{1}{M_C} + \frac{1}{2M_H}\right)\frac{r^2}{Z^2} \qquad [4.14]$$

where M_O, M_C, M_H are the masses of oxygen, carbon and hydrogen respectively; and

Z is the distance from the carbon to the H-H line.

The Isotope Effect

The potential energy function for two molecules containing different atomic isotopes are similar to a high degree of approximation. The difference in mass of the two isotopes, however, affects the vibrational and rotational energy levels associated with the electronic states of the molecule. For isotopic molecules, the origin band of an electronic transition has the same profile, but since w, x (equation [4.2]) are mass dependent[73] the vibrational bands will be displaced by the amount:

$$\Delta\nu = \sum_i w_i'\left(v_i'+\tfrac{1}{2}\right) + \sum_i \sum_{k>i} x_{ik}'\left(v_i'+\tfrac{1}{2}\right)\left(v_k'+\tfrac{1}{2}\right) - \left[\sum_i w_i'^*\left(v_i'+\tfrac{1}{2}\right) + \sum_{ik}\sum x_{ik}'^*\left(v_i'+\tfrac{1}{2}\right)\left(v_k'+\tfrac{1}{2}\right)\right.$$

$$\left. - \sum_i w_i''\left(v_i''+\tfrac{1}{2}\right) - \sum_i \sum_{k>i} x_{ik}''\left(v_i''+\tfrac{1}{2}\right)\left(v_k''+\tfrac{1}{2}\right) - \left[-\sum_i w_i''^*\left(v''+\tfrac{1}{2}\right) - \sum_i \sum_{k>i} x_{ik}''^*\left(v_i''+\tfrac{1}{2}\right)\left(v_k''+\tfrac{1}{2}\right)\right]\right] \qquad [4.15]$$

for each normal vibration.

Chlorine has two stable isotopes - chlorine 35 with a relative abundance of 75.53% and chlorine 37 with a relative abundance of 24.47[69]. Three isotopic thiocarbonyl dichlorides are thus possible: $C\ell^{35}C\ell^{35}CS$, $C\ell^{37}C\ell^{37}CS$, and $C\ell^{35}C\ell^{37}CS$. From the relative abundances one can calculate that the three compounds will be found naturally in the ratio of 9:6:1, respectively. The vibrational spectra of each of the three compounds will be identical except that the bands will be displaced from one another in the spectrum. The isotopic shift is generally greatest in bands that result from transitions due to

vibrations involving large amplitude of motion of the chlorine atoms.

Brand et al.[15] in their studies of $^1A_2 \leftarrow {}^1A_1$ transition of $C\ell_2CS$ and Balfour[87] in his investigation of oxalyl chloride have found that the isotopic splitting was a linear function of the number of quanta of the vibration excited in one of the combining electronic states.

CHAPTER 5

THE $^1A_1 \leftarrow {}^1A_1(\pi \rightarrow \pi^*)$ SYSTEM OF $C\ell_2CS$

Sample Preparation

$C\ell_2CS$ is a red liquid at room temperature with a vapour pressure of 76 mm Hg[76]. The $C\ell_2CS$ used to obtain spectra was obtained from two sources. Mr. I. Brindle prepared $C\ell_2CS$ using the following reaction[77]:

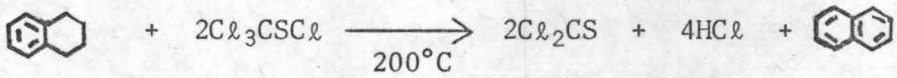

Near the completion of this work, $C\ell_2CS$ was purchased from the Aldrich Chemical Company. It was found that $C\ell_2CS$ obtained from both sources contained SO_2. The SO_2 was removed by a trap-to-trap distillation under vacuum at room temperature and degassing the bulk sample prior to filling an absorption cell. The bulk sample was stored at room temperature, and was stored in the dark when left for long periods of time. This prevented the formation of $C\ell_2CS$ dimer (a white solid).

Low Resolution Absorption Spectra

This author has previously recorded the spectrum of the $^1A_1 \leftarrow {}^1A_1(\pi \rightarrow \pi^*)$ system and the unknown system with a Cary 14 double beam recording spectrometer[18]. These two systems were re-examined using a 1.5 m Bausch and Lomb model 11 grating spectrograph in the first order. The spectrograph in first order has a dispersion of 15 Å/mm and a resolving power of 35,000.

A 450 watt Xenon lamp source was used in all cases. The system was recorded using slit widths between 32 and 60 microns. A ten cm gas absorption cell with an attached cold finger were used to contain the sample. Vapour pressures of 10 mm Hg or less were obtained by cooling the finger with ice or solid carbon dioxide. It was found that exposures up to four hours were needed to record as much of the system as possible. The Long exposures with large

slit widths resulted in the clouding of the film due to stray light. SO_2 bands were often present in the spectrum after long exposures of the sample to the light source.

The unknown system was photographed using a slit width of 10 microns. Vapour pressures of 20 mm Hg and less were found to produce the best results. A 1.8 m White type multiple reflection cell[78] was used to give path lengths of up to 10 metres. Photographs were obtained at both room temperature and -78°C[69].

All spectra were recorded on Kodak Spectrum Analysis No. 1 film. Developing and fixing were done in the prescribed way.

High Resolution Spectra

High resolution spectra of the unknown system were obtained using a 20-foot Ebert grating spectrograph, and a 450 watt Xenon arc light source. Exposure times of between fifteen minutes and one and one-half hours were used with a slit width of 40 microns. All spectra were obtained at room temperature using an absorption path length of one metre and gas pressures of between one and fifty mm Hg. Spectrum Analysis No. 1 film was used, with standard developing procedures.

Attempts were made to photograph the $^1A_1 \leftarrow {}^1A_1(\pi \rightarrow \pi^*)$ system under high resolution. It was found that exposures of up to ten hours with a slit width of sixty microns was insufficient to photograph any of the $^1A_1 \leftarrow {}^1A_1$ $(\pi \rightarrow \pi^*)$ system. Similar difficulties have been found by C.R. Subramaniam in photographing the $^1A_1 \leftarrow {}^1A_1(\pi \rightarrow \pi^*)$ system of C&FCS[72].

Iron emission lines, produced by an iron arc, were used as reference lines to calculate the wavenumbers of the spectral features. Wherever possible a least squares fit of the iron arc lines was used to calculate the wavenumbers of the bands. The wavenumber values of these features thus have an error of

± 0.5 cm^{-1}. Microdensitometer traces were taken and wavenumbers obtained by interpolation for bands at the red end of the unknown system and for the bands of the $^1A_1 \leftarrow {}^1A_1(\pi \rightarrow \pi^*)$ system. These wavenumber values have an error of ± 5 cm^{-1}.

The $^1A_1 \leftarrow {}^1A_1(\pi \rightarrow \pi^*)$ System of $C\ell_2CS$

The $^1A_1 \leftarrow {}^1A_1(\pi \rightarrow \pi^*)$ system of $C\ell_2CS$ extends from 2800 Å to 2300 Å, reaching a maximum at approximately 2550 Å. It is the most intense system of $C\ell_2CS$ yet to be studied, having an oscillator strength of 5.90×10^{-2} in the gas phase. Fig. 5.1 shows the $^1A_1 \leftarrow {}^1A_1(\pi \rightarrow \pi^*)$ system of $C\ell_2CS$ recorded using a Cary 14 spectrometer. The transition appears as discrete vibrational structure (especially at the red end of the transition) superimposed on a continuum of rapidly increasing intensity towards higher frequencies. The small difference in intensity between the vibrational structure and the background itself is the cause of the experimental difficulties encountered in photographing the transition. It was this profile that led early investigators to label the transition as dissociative.

Fig. 5.2 shows the section of the $^1A_1 \leftarrow {}^1A_1(\pi \rightarrow \pi^*)$ system that has been recorded using the Bausch and Lomb spectrograph. Fig. 5.2 is a microdensitometer trace of the $^1A_1 \leftarrow {}^1A_1(\pi \rightarrow \pi^*)$ system. All of the bands in the system are red degraded. Table 5.1 lists the features that have been assigned to the $^1A_1 \leftarrow {}^1A_1(\pi \rightarrow \pi^*)$ transition, the proposed assignment, polarizations and intensities.

In the $^1A_1 \leftarrow {}^1A_1$ spectrum, four ground state frequencies are identified: ν_1'' (1142 cm^{-1}), ν_2'' (500 cm^{-1}), ν_3'' (290 cm^{-1}) and ν_4'' (475 cm^{-1}). Most of the bands up to 36299 cm^{-1} can be accounted for by using these frequencies. The band at 36045 cm^{-1} is a notable exception. The difficulty in assigning the band at 36045 cm^{-1} and accounting for its intensity led this investigator to

Fig. 5.1

$^1A_1 \leftarrow {}^1A_1(\pi \rightarrow \pi^*)$ System of $C\ell_2CS$

Recorded on a Cary 14 Spectrometer

experimental conditions

room temperature

10 cm cell

26 mm Hg gas pressure

2.5 Å/sec chart speed

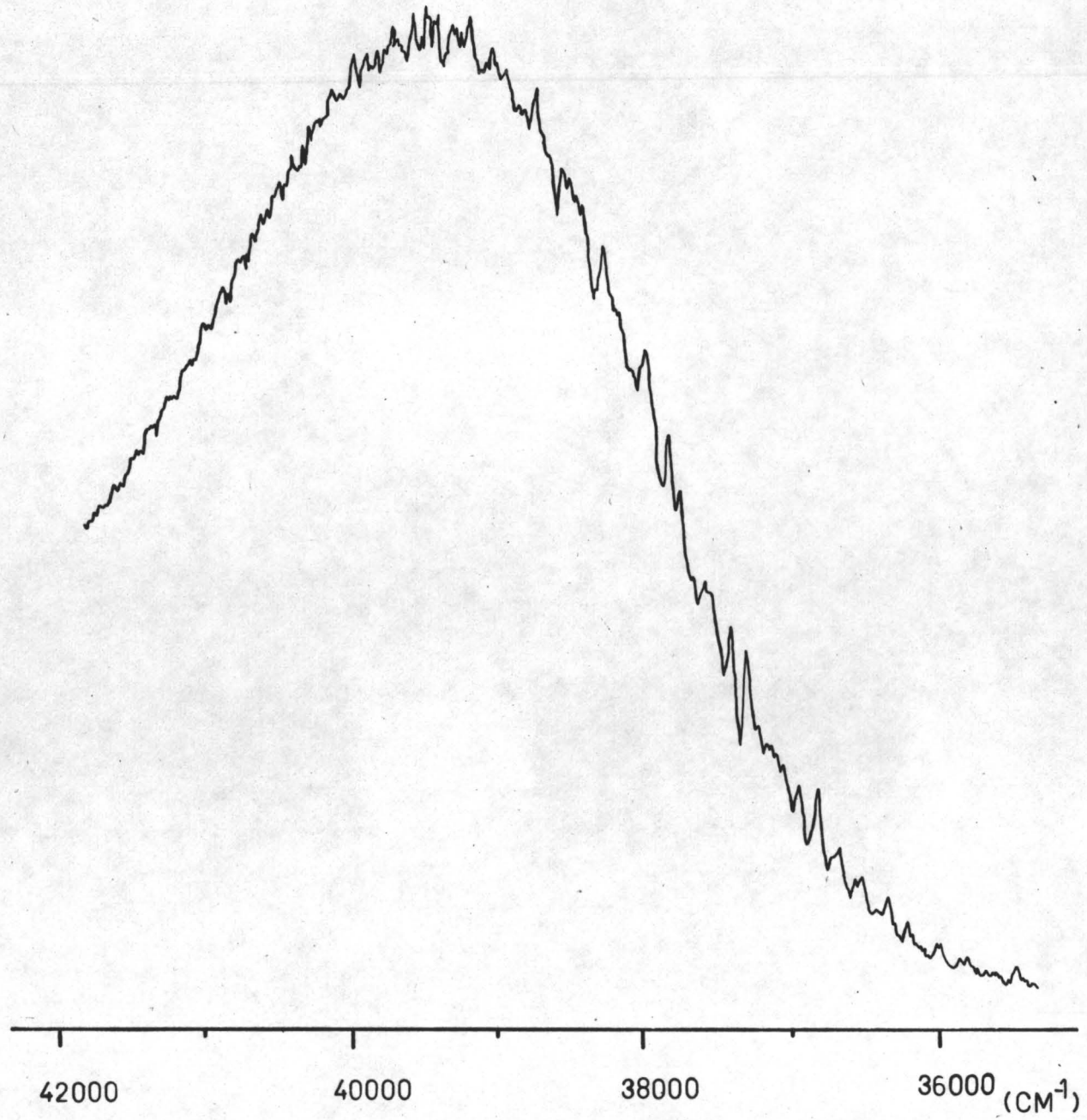
42000
40000
38000
36000 (CM-1)

Fig. 5.2

$^1A_1 \leftarrow {}^1A_1(\pi \rightarrow \pi^*)$ System of $C\ell_2CS$,

Microdensitometer Trace of a Bausch and Lomb Plate

experimental conditions

room temperature

10 cm cell

<1 mm Hg gas pressure

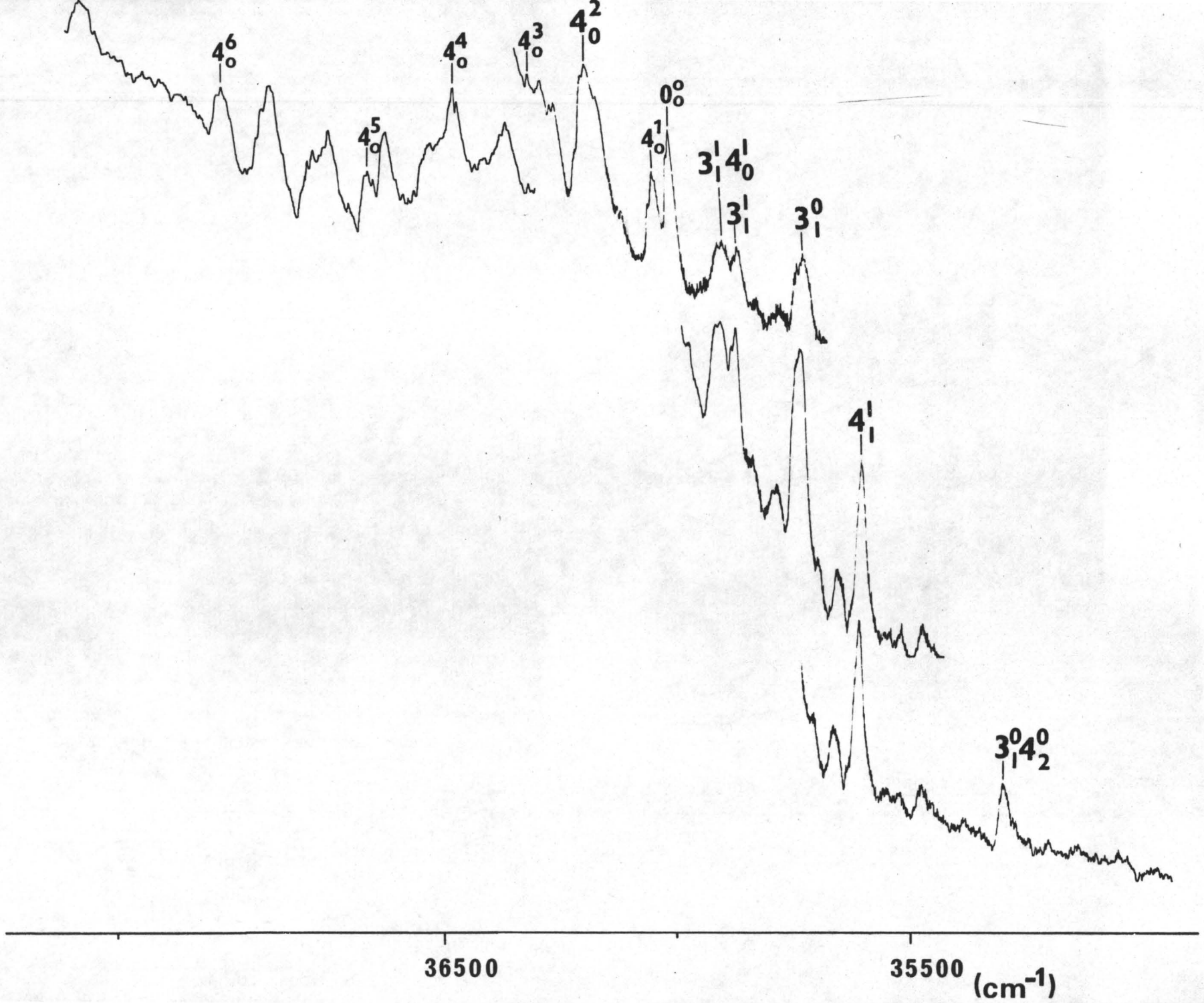
4_0^6
4_0^5
4_0^4
4_0^3
4_0^2
4_0^1
0_0^0
$3_1^1 4_0^1$
3_1^1
3_1^0
4_1^1
$3_1^0 4_2^0$
36500
35500
(cm^{-1})

Table 5.1

Band Frequencies, Assignments, Polarizations and Intensities of the $A_1 \leftarrow {}^1A_1(\pi \rightarrow \pi^*)$ Transition

Frequency (cm^{-1})	Assignment[†]	Polarization	Intensity[*]
37225			s
37166	$3_0^6 4_0^3$?		vw
37156	$4_0^8(4^+)$		vw
37100			vw
37089			vw
37070			vw
37059			vw
37028	$3_0^5 4_0^3$		w
36981	$1_0^1 4_0^3$		s
36966	$4_0^7(3^-)$		s
36890			sh
36880	$3_0^4 4_0^3$		s
36860	$1_0^1 4_0^2$		vs
36783	$4_0^6(3^+)$		s
36766	$3_0^2 4_0^4$(?)		s
36749			s
36734	$3_0^3 4_0^3$		vs
36720	$1_0^1 4_0^1$		
36688	$0_0^0 1_0^1$		w
36646	$4_0^5(2^-)$		s
36607	$3_0^1 4_0^4$		vs
36588	$3_0^2 4_0^3$		
36513	$1_0^1 4_1^3$		s

Frequency (cm^{-1})	Assignment	Polarization	Intensity*
36490			w
36461	$4_0^4(2^+)$		vs
36453	$3_1^3 4_0^3$		s
36439	$3_0^1 4_0^3$		sh
36395	$1_0^1 2_0^1 4_1^1$		w
36347		x	s
36340	$3_0^2 4_0^1$		sh
36299	$4_0^3(1^-)$	z	w
36272			w
36252	$1_0^1 4_1^1$		w
36244			w
36192	$3_0^1 4_0^1$		sh
36183	$4_0^2(1^+)$	z	w
36156	$3_2^1 4_0^1$		sh
36045	$4_0^1(0^-)$	x	s
36007	$0_0^0(0^+)$	z	s
35961	$2_1^0 4_0^4$		sh
35942			vw
35899	$3_1^1 4_0^1$	x	w
35864	$0_0^0 3_1^1$		w
35822	4_1^3		vw
35770	$3_1^0 4_0^1$	x	vw
35724	$0_0^0 3_1^0$	z	w
35673	$2_1^0 3_1^0 4_0^4$		vw
35628	$3_2^1 4_0^1$	x	vw
35570	4_1^1	z	w

Frequency (cm^{-1})	Assignment	Polarization	Intensity*
35505	$0_0^0 2_1^0$		vw
35480	$3_3^0 4_0^1$	x	vw
35432	$0_0^0 3_2^0$	z	w
35342	4_2^3		vw
35338	$3_3^1 4_0^1$		vw
35257	$0_0^0 3_1^0 4_1^0$	x	w
35214	$0_0^0 2_1^0 3_1^0$		sh
35167	$2_2^0 3_1^0 4_0^4$		vw
35109	4_2^1	x	vw
35069	$2_1^0 4_1^1$		vw
35865	$0_0^0 1_1^0$		vw
34784	$0_0^0 3_1^0 4_2^0$		vw

*vs very strong

s strong

w weak

vw very weak

sh shoulder

†alternate notation in brackets

use a Coon double-minimum potential function for the inversion motion. It was assumed that the bands at 36007 cm^{-1} and 36045 cm^{-1} were the 0^+ (0_0^0) and 0^- (4_0^1) energy levels of ν_4' and attempts were made to account for bands to the blue of 36045 cm^{-1} as arising from transition to the 1^+, 1^-, etc., levels in the excited state. It was found that the bands at 36183 cm^{-1} and 26299 cm^{-1} could be easily accounted for using a wide range of ρ and B values (see Table 5.2). When ρ = 0.60 and B = 0.60, the bands further to the blue agreed most closely (in frequency) to those found experimentally. Brand et al.[15] also found that ρ = 0.6 gave the best results in the $^1A_2(\pi^*,n)$ state, although the observed $4\nu_4'$ and $5\nu_4'$ energy levels differed significantly from the calculated values. The assignment of 36007 cm^{-1} and 36045 cm^{-1} as resulting from transitions to the 0^+ and 0^- energy levels (respectively) was confirmed by following experimental evidence. If the excited state could be assigned to the C_{2v} point group (an assumption made by Brand et al.[15] due to the low barrier to inversion) the 0^+ level would have a_1 symmetry, while the 0^- level would have b_1 symmetry (see Fig. 5.3). The vibrational selection rule (see equation [4.6]) would predict that the transition to the 0^+ level should be more intense than the transition to the 0^- level since the transition to the 0^- level must borrow intensity from a nearby transition of proper symmetry. Also since the transition is allowed electronically, the origin band should be intense. These two characteristics of the origin band are found experimentally. The transition to the 0^+ level should be z polarized, while the transition to the 0^- level should be x polarized. The spectra obtained using the Bausch and Lomb spectrograph are of high enough dispersion to show that the bands at 36007 cm^{-1} and 36045 cm^{-1} do have different profiles. The 36007 cm^{-1} band appears as two sharp "heads", the lower frequency head being the more intense. The 36045 cm^{-1} band appears to be less sharp, having a weak head in

Fig. 5.3

Vibrational Transitions Between the Ground and $A_1(\pi^*,\pi)$ Excited State of $C\ell_2CS$

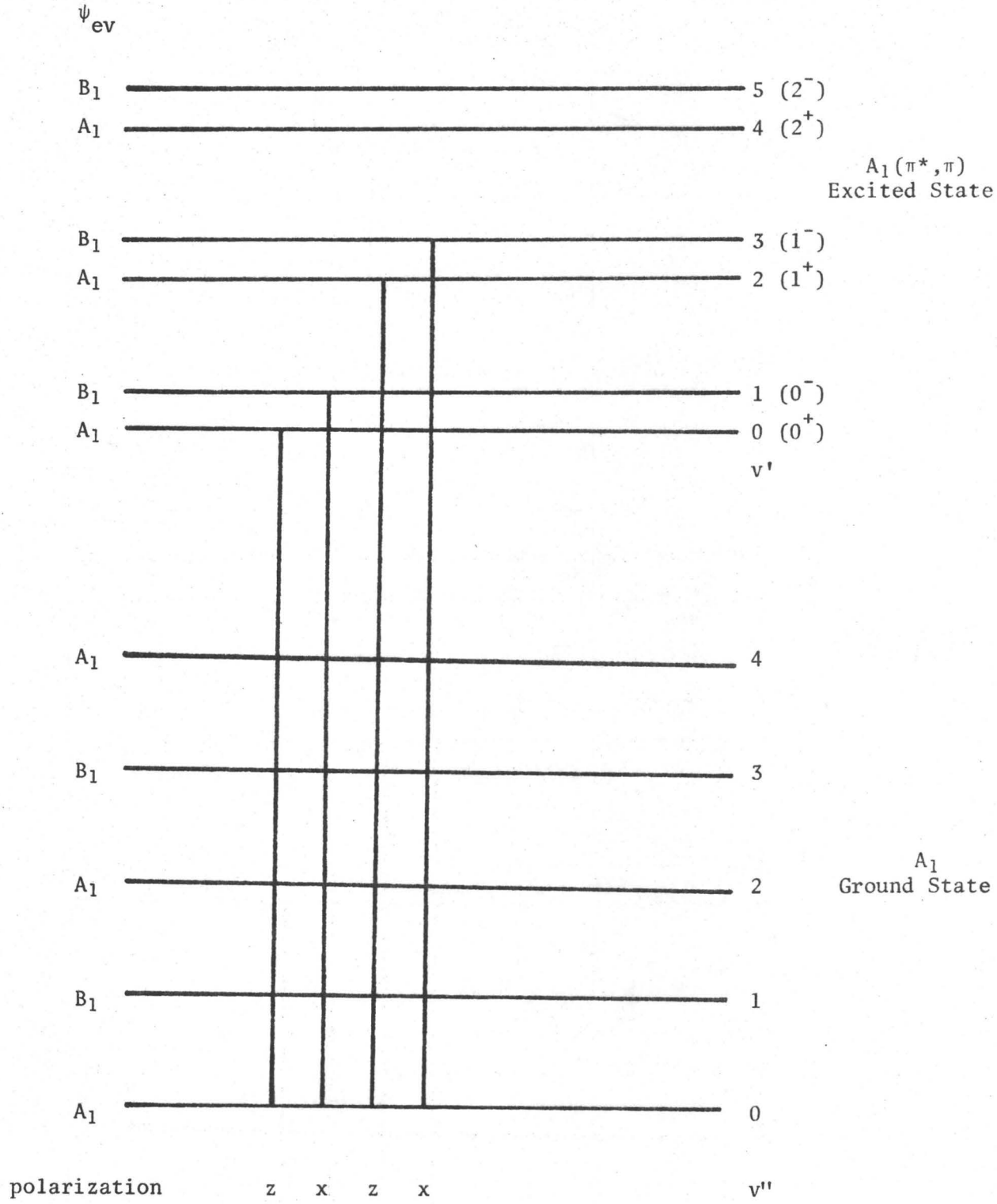

the middle of a weak broad band. The band at 36007 cm^{-1} was assumed to be a typical z polarized band and the band at 36045 cm^{-1} was assumed to be a typical x polarized band, and the polarization of the other bands in the spectrum were determined (where possible) by comparison to these two (see Table 5.1). A final confirmation of the 0^+, 0^- assignment came by comparing the vibrational pattern originating from the 0^+, 0^-, 1^+, 1^- bands. Onto the 0^+ and 1^+ bands are attached one quantum of ν_2'' and then one (or two in the case of 0^+) quantum of ν_4''. Onto the 0^- and 1^- bands are attached two quanta of ν_4'' vibration. Onto the 0^+, 0^-, 1^+ and 1^- bands one quantum of ν_1' can be added, and the bands originating from the 0^- and 1^- bands are stronger than the bands originating from the 0^+ and 1^+ bands.

Three excited state frequencies were also assigned: $\nu_1' = 680\ cm^{-1}$, $\nu_3' = 143\ cm^{-1}$ and $\nu_4' = 185\ cm^{-1}$. The ν_4' value was obtained from the Coon calculation. The first few quanta show irregular frequency separations, but as more quanta were excited they converge on 185 cm^{-1} (see Table 5.2). Brand et al.[15] assigned $\sim$150 cm^{-1} as ν_4' in the $^1A_2 \leftarrow {}^1A_1(n \rightarrow \pi^*)$ transition of $C\ell_2CS$ using Coon's method.

The large drop in frequency in both ν_4 (carbon-sulphur stretch) and ν_3 (carbon-chlorine stretch) can be explained by making use of the molecular orbitals generated using the CNDO-PD program. As can be seen in Table 5.3, on comparing the π orbital to the π^* orbital, the latter contains a node between the carbon and the sulphur atoms. Also on going from the π to the n to the π^* orbital, the contribution to the molecular orbitals by the chlorine atoms decreases allowing the $C\ell$-C-$C\ell$ angle to open. An excited state with a longer carbon-sulphur bond and longer carbon-chlorine bond does not seem unreasonable.

The out-of-plane angle in the excited state has been calculated to be

Table 5.2

Energy Levels of ν_4'

Assignment	Observed (cm^{-1})	Calculated		
		$\rho = .6$ B = .6	$\rho = .9$ B = .767	$\rho = 1.2$ B = .92
0^+ (0)	0 (37007)[a]	0	0	0
0^- (1)	38 (36045)[a]	38	37	38
1^+ (2)	176 (36183)[a]	176	173	176
1^- (3)	292 (36299)	305	294	289
2^+ (4)	454 (36461)	458	437	423
2^- (5)	639 (36646)	621	586	558
3^+ (6)	776 (36783)	793	739	697
3^- (7)	959 (36966)	971	897	840
4^+ (8)	1149 (37156)	1154	1056	980
4^- (9)	-	1340	1217	1123
Barrier Height (cm^{-1})		125	130	135
Q_m		.933	.978	.989
Angle (θ)		26.6°	22.6°	22.8°

[a]data on which calculations were based

Table 5.3

Molecular Orbital Coefficients of $C\ell_2CS$*

CARBON	π	n	π^*
2s	.0000	.0000	.0000
$2p_x$	.3701	.0000	.4929
$2p_y$	.0000	.2139	.0000
$2p_z$	.0000	.0000	.0000
SULPHUR			
3s	.0000	.0000	.0000
$3p_x$	.5692	.0000	-.7359
$3p_y$	.0000	-.8268	.0000
$3p_z$	.0000	.0000	.0000
$3d_{z^2}$	.0000	.0000	.0000
$3d_{xz}$	-.1945	.0000	-.2695
$3d_{yz}$	.0000	-.1273	.0000
$3d_{x^2-y^2}$	.0000	.0000	.0000
$3d_{xy}$	.0000	.0000	.0000
CHLORINE			
3s	.0000	-.0553	.0000
$3p_x$	-.4894	.0000	-.1401
$3p_y$	.0000	-.3290	.0000
$3p_z$	.0000	.1101	.0000
$3d_{z^2}$	.0000	.0075	.0000
$3d_{xz}$	.0721	.0000	.1201
$3d_{yz}$	.0000	-.0605	.0000
$3d_{x^2-y^2}$	.0000	-.0117	.0000
$3d_{xy}$	-.0766	.0000	-.1933

*obtained from CNDO-PD program. Geometry same as listed in Table 2.3.

26.6° (see Table 5.2). This is consistent with the angle (33°) calculated by Brand et al.[15] for the $^1A_2(n,\pi^*)$ state, although the barrier to inversion for the $^1A_1(\pi^*,\pi)$ state was calculated to be 20% of the value calculated for the $^1A_2(n,\pi^*)$ state (597 cm^{-1}).

Difficulty was encountered in assigning the bands to the blue of 36981 cm^{-1}. This was probably a result of the weakness and broadness of the bands. It is possible that these bands are hot bands originating from bands to the blue that have not been photographed.

The bands at 35899 cm^{-1} and 35864 cm^{-1} are assigned as sequence bands 3_1^1. This assignment is made because of the remarkable similarity of profiles between these two bands and the bands at 36045 cm^{-1} and 36007 cm^{-1} (respectively). Since the polarization of the bands remains the same, they must be related by a totally symmetric vibration. The assignment of 3_1^1 is consistent with this reasoning.

CHAPTER 6

THE UNKNOWN SYSTEM OF $C\ell_2CS$

Between the strong $^1A_1 \leftarrow {}^1A_1(\pi \rightarrow \pi^*)$ system and the weak $^{1,3}A_2 \leftarrow {}^1A$ $(n \rightarrow \pi^*)$ systems lies a weak system (experimental oscillator strength of 2.42×10^{-5}[18]) which has been referred to as the "unknown system". The energy and oscillator strength calculations carried out in Chapter 2 would lead to the conclusion that the transition could be $B_1 \leftarrow {}^1A_1(\sigma \rightarrow \pi^*)$, since the intensity of the transition is much less than the $^1A_1 \leftarrow {}^1A_1(\pi \rightarrow \pi^*)$ transition. A recent paper by D. Chadwick[86] on the photoelectron spectra of phosgene and thiophosgene has provided additional evidence that may be used to identify this unknown transition. By means of photoelectron spectroscopy, Chadwick was able to list the bonding orbitals of $C\ell_2CS$ in order of energy. The results of these experiments can be seen in Fig. 6.1. Chadwick's results indicate that the sulphur n electron is the least tightly bound of the $C\ell_2CS$ electrons. Next is the pi electron in the thiocarbonyl group. These are followed by 3 non-bonding (n) electrons on the chlorine atom. One n electron is in an atomic orbital with b_2 symmetry, one with a_2 symmetry and one with a_1 symmetry. These chlorine n electrons have very similar energy (both calculated by CNDO and experimental). Up to this point the molecular orbital labels (σ, π, n, σ^*, π^*) have been assigned on the basis of a description of the atomic orbitals in the C-S group. Thus the molecular orbital described as σ could also be described as $n_{C\ell}$ depending upon whether the atomic orbitals on the C-S on the $C\ell$'s are considered.

There are three possible transitions combining the chlorine n electron and the π^* orbital:

Fig. 6.1

Molecular Orbitals of $C\ell_2CS$

Energy (eV)	Symmetry	Description
9.84	b_2	sulphur lone pair
10.65	b_1	C-S pi electron
11.96	b_2	chlorine lone pair
12.38	a_2	chlorine lone pair
12.69	a_1	chlorine lone pair
14.47	a_1	$CC\ell_2$ stretching mode
15.11	b_1	chlorine lone pair
16.19	b_2	σ bonding
18.25	a_1	σ bonding

	$f_{calculated}$
$A_2 \leftarrow {}^1A_1(\pi^*, n_{C\ell})$	0
$B_2 \leftarrow {}^1A_1(\pi^*, n_{C\ell})$	3.2×10^{-3}
$B_1 \leftarrow {}^1A_1(\pi^*, n_{C\ell})$	3.8×10^{-3}

Transitions from the n orbitals to the σ^* orbital have not been considered because of the energy involved in such transitions.

The first transition is formally forbidden, but the second and third are allowed. Because of the very low oscillator strength value observed in the unknown system, the label $A_2 \leftarrow {}^1A_1(n \rightarrow \pi^*)$ is most suitable. CNDO calculations of the type used in Chapter 2 show that the calculated oscillator strength is zero. The transition energy is calculated to be 50050 cm^{-1} (1998 Å).

A possible confirmation of this labelling could be the assignment of a second $^1A_2 \leftarrow {}^1A_1(n \rightarrow \pi^*)$ transition in F_2CO by Workman and Duncan[42]. This second $^1A_2 \leftarrow {}^1A_1(n \rightarrow \pi^*)$ transition was approximately as intense as the first transition and had an energy greater than the first $^1A_2 \leftarrow {}^1A_1(n \rightarrow \pi^*)$ transition but less than the $^1A_1 \leftarrow {}^1A(\pi \rightarrow \pi^*)$ transition. Unfortunately a more detailed comparison cannot be made since the photoelectron data for F_2CO is not available.

The Spectrum of the $A_2 \leftarrow {}^1A_1(n \rightarrow \pi^*)$ Transition in $C\ell_2CS$

The spectrum of this transition extends from 3470 Å to approximately 2950 Å with a maximum at 3180 Å. Fig. 6.2 shows the spectrum as recorded on a Cary 14 spectrophotometer. As can be seen from Fig. 6.2 there appear to be two types of bands in the spectrum. At the red end are broad weak bands that appear to merge into a set of sharper more intense bands that extend to the blue of the transition. This description is similar to the one given to the $A_2 \leftarrow {}^1A_1$ transition of $C\ell_2CS$, where the differences have been attributed

FIG. 6.1

The Unknown System of Cl_2CS

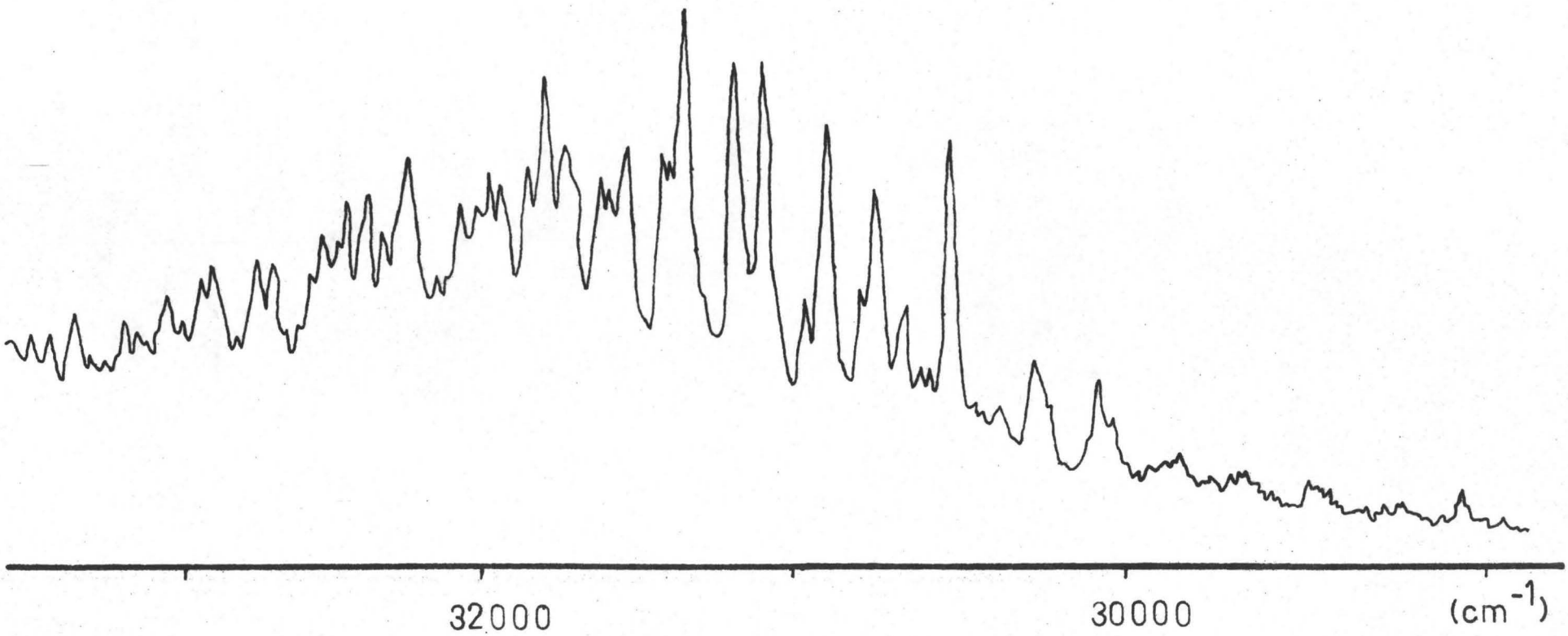

to the singlet and triplet component of the transition. At this point, there is no evidence other than the gross structure of the system, to justify the conclusion that the bands between 3470 Å and 2950 Å are due to the singlet and triplet components. Work on the analysis of the system was concentrated on the red end of the system. Fig. 6.2 shows a microdensitometer trace of the spectrum obtained using a Baush and Lomb spectrometer for the region 33150 cm^{-1} to 29000 cm^{-1}. Appendix E lists the wavenumbers, relative intensities and possible assignments for the bands in this region. Becuase of the weakness of most of the bands in this region, it was necessary to use interpolation on the microdensitometer traces to assign the wavenumber of many bands. The wavenumbers and intensities of bands at the blue end of the spectrum are listed in Appendix D.

In the spectrum five ground state frequencies were observed: ν_1'' (1141 cm^{-1}), ν_2'' (500 cm^{-1}), ν_3'' (289 cm^{-1}), ν_4'' (475 cm^{-1}) and ν_5'' (817 cm^{-1}). ν_2'' was the most active frequency in the spectrum that was analysed. 640 cm^{-1} has been assigned as an excited state frequency. Four bands (29948 cm^{-1}, 29874 cm^{-1}, 29849 cm^{-1} and 29465 cm^{-1}) have one quantum of ν_1'', ν_2'', ν_4'' and ν_5'' attached to them (see Table 6.1). Onto these bands are attached bands separated by $\sim$640 cm^{-1}. This "excited state vibration" also seemed to be more active in the blue part of the spectrum that was analysed.

Although no attempt had been made to analyse any of the spectra at the extreme blue end of the unknown system, it was evident from the prints made from Ebert plates that an isotope effect could be seen in many of the bands. In most cases, only the bands due to the 35-35 and 35-37 isotopes could be seen.

Table 6.1

Frequency Differences in the Unknown System of $C\ell_2CS$

	29948 (cm^{-1}) (A)	29874 (cm^{-1}) (B)	29849 (cm^{-1}) (C)	29465 (cm^{-1}) (D)
$-\nu_1''$	28807 (1141 cm^{-1})	-	-	-
$-\nu_2''$	29449 (499 cm^{-1})	29374 (500 cm^{-1})	29349 (500 cm^{-1})	28958 (507 cm^{-1})
$-\nu_4''$	-	29407 (467 cm^{-1})	29374 (475 cm^{-1})	28993 (472 cm^{-1})
$-\nu_5''$	29134 (814 cm^{-1})	29053 (816 cm^{-1})	29030 (819 cm^{-1})	-
	A - ν_2''	B - ν_2''	C - ν_2''	D - ν_2''
+640	30089 (638 cm^{-1})	-	-	29601 (643 cm^{-1})
	A - ν_4''	B - ν_4''	C - ν_4''	D - ν_4''
+640	-	30056 (649 cm^{-1})	-	-
	A - ν_5''	B - ν_5''	C - ν_5''	D - ν_5''
+640	29775 (641 cm^{-1})	29695 (642 cm^{-1})	29030 (644 cm^{-1})	-

REFERENCES

1. Kolbe, Ann. 45, 44 (1843).
2. V. Henri, Structure des Molecules (Hermann and Cie, Paris, 1925).
3. H. W. Thompson, Trans. Roy. Soc. 251 (1941).
4. C. Bailey and J. Hale, Phil. Mag., 25, 98 (1938).
5. J. Duschesne, J. Chem. Phys. 21, 548 (1952).
6. V. Henri, J. Duchesne, Nature 143, 28 (1939).
7. L. Burnelle, Physics 24, 620 (1956).
8. McMurry, J. Chem. Phys. 9, 231 (1941).
9. J. C. D. Brand, J. Chem. Soc. 858 (1956).
10. J. C. D. Brand, J. Callomon, J. K. G. Watson, Disc. Faraday Soc. 35, 175 (1963).
11. J. C. D. Brand, Williamson, Disc. Faraday Soc. 35, 184 (1963).
12. L. O. Brockway, J. Y. Beach, L. Pauling, J. Am. Chem. Soc., 57, 2693 (1935).
13. H. W. Thompson, J. Chem. Phys. 6, 248 (1938); Trans. Faraday Soc. 37, 251 (1947).
14. Downs, Spectrochim. Acta, 19, 1165 (1963).
15. J. C. D. Brand, J. H. Callomon, D. C. Moule, J. Tyrrell, T. H. Goodwin, Trans. Faraday Soc., 61, 2365 (1965).
16. D. C. Moule, C. R. Subramaniam, Chem. Comm. 1340 (1969).
17. J. Fabian, H. Viola, R. Mayer, Tetrahedron 23, 4323 (1967).
18. E. Farnworth, B.Sc. Thesis, Brock University, St. Catharines (1970).
19. Shoemaker and Garland, Experiments in Physical Chemistry, McGraw-Hill Book Co., N.Y. (1962).
20. Harrison, Lord, Loofbourow, Practical Spectroscopy, Prentice-Hall Inc., Englewood Cliffs, N.J. (1963).
21. H. Suzuki, Electronic Absorption Spectra and Geometry of Organic Molecules, Academic Press (1967).
22. Einstein (1917), from ref. 34.

23. R. S. Mulliken, J. Chem. Phys. 7, 14 (1939).

24. H. Jaffé and Orchin, Theory and Applications of Ultraviolet Spectroscopy, John Wiley and Sons Inc., N.Y. (1962).

25. G. Herzberg, Spectra of Diatomic Molecules, D. van Nostrand Co. Inc., N.J. (1966).

26. J. C. Slater, Phys. Rev. 36, 57 (1930).

27. R. M. Hochstrasser, Molecular Aspects of Symmetry, W. A. Benjamin Inc., New York (1966).

28. Janet Del Bene, H. H. Jaffé, J. Chem. Phys. 48, 1807 (1968).

29. Stevenson, Lu Valle, Schoemaker, J. Am. Chem. Soc. 61, 2508 (1939).

30. V. W. Laurie, D. T. Pence, J. H. Jackson, J. Chem. Phys. 37, 2996 (1962).

31. G. W. Robinson, J. Chem. Phys. 21, 1741 (1953).

32. Donald R. Johnson, Francis X. Powell, William H. K. Kirchhoff, J. Molec. Spectrosc. 39, 136 (1971).

33. Reference (15).

34. G. W. King, Spectroscopy and Molecular Structure, Holt, Rinehart and Winston Inc., N.Y. (1965).

35. Claude Giessner-Prettre, Alberte Pulleman, Theoret. Chim. Acta. (Berl.) 13, 265 (1969).

36. G. W. Robinson, V. E. DiGiorgio, J. Chem. Phys. 28, 1678 (1958).

37. S. E. Hodges, J. R. Henderson, J. B. Coon, J. Molec. Spectrosc. 2, 99 (1958).

38. J. C. D. Brand, J. Chem. Soc., 858 (1956).

39. G. W. Robinson, V. E. DiGiorgio, Can. J. Chem., 36, 31 (1958).

40. W. C. Price, J. Chem. Phys. 3, 256 (1935).

41. G. Fleming, M. M. Anderson, A. J. Harrison, and L. W. Pickett, J. Chem. Phys., 30, 351 (1959).

42. G. L. Workman, A. B. F. Duncan, J. Chem. Phys., 52, 3204 (1970).

43. D. C. Moule, P. D. Foo, J. Chem. Phys. 55, 1262 (1971).

44. D. C. Moule, A. K. Mehra, J. Molec. Spectrosc. 35, 137 (1970).

45. D. C. Moule, Can. J. Chem. 48, 2623 (1970).

46. C. Drury, B.Sc. Thesis, Brock University, St. Catharines (1972).

47. Reference (16).

48. H. W. Kroto, D. P. Santry, J. Chem. Phys. 47, 792 (1967).

49. L. C. Cusachs, B. L. Trus, J. Chem. Phys. 46, 1532 (1967).

50. Obtained from Quantum Chemistry Program Exchange,Chemistry Dept., Indiana University, U.S.A.

51. L. Burnelle, M. J. Kranepool, J.Molec. Spectrosc. 37, 383 (1971).

52. W. A. Yeranos, Z. Naturforschg. 21a, 1864 (1966).

53. J. A. Pople and D. L. Beveridge, Approximate Molecular Orbital Theory, McGraw-Hill Book Co., N.Y. (1970).

54. H. Sponer and E. Teller, Rev. Mod. Phys., 13, 75 (1941).

55. I. Zanon, G. Giacometti, D. Picciol, Spectrochim. Acta 19, 301 (1963).

56. This work.

57. E. B. Wilson, J. C. Decius, P. C. Cross, Molecular Vibrations, McGraw-Hill Book Co. Inc., New York (1955).

58. S. P. McGlynn, T. Azumi, M. Kinoshita, Molecular Spectroscopy of the Triplet State, Prentice-Hall, New Jersey (1969).

59. D. Bohm, Quantum Chemistry, Prentice Hall, Englewood Cliffs, New Jersey (1951).

60. J. A. Pople, J. W. Sidman, J. Chem. Phys. 27, 1270 (1957).

61. H. Longuett-Higgens, Proc. Roy. Soc. (London), A 235, 537 (1956).

62. J. A. Pople, G. A. Segal, J. Chem. Phys. 43, 5136 (1965).

63. J. A. Pople, D. P. Santry, G. A. Segal, J. Chem. Phys. 43, 5129 (1965).

64. J. A. Pople, G. A. Segal, J. Chem. Phys. 44, 3289 (1966).

65. Core Physical Chemistry Notes, McMaster University (1970).

66. R. Pariser, R. G. Parr, J. Chem. Phys. 21, 767 (1953).

67. N. Mataga and N. Nishimoto, Z. Phys. Chem. (Frankfurt), 13, 140 (1957).

68. A. van Putten, Private Communication.

69. Handbook of Chemistry and Physics, 49th Edition, R. Weast Editor, The Chemical Rubber Co., Cleveland, Ohio (1968).

70. I. C. Hisatsune, D. F. Eggers Jr., J. Chem. Phys. 23, 487 (1955).

71. J. Overend, J. R. Scherer, J. Chem. Phys. 32, 1289 (1960).

72. C. R. Subramaniam, Private Communication.

73. G. Herzberg, Electronic Spectra of Polyatomic Molecules, D. van Nostrand Co. Inc., New Jersey (1966).

74. J. N. Murrell, J. A. Pople, Proc. Phys. Soc. (London), A69, 245 (1956).

75. S. Durmay, J. N. Murrell, J. M. Taylor, R. Suffolk, Mol. Phys. 19, 533 (1970).

76. N. Kharasch, C. Meyers, The Chemistry of Organic Sulphur Compounds, Pergamon Press, London (1966).

77. E. Tietze, S. Peterson, Ger. Patent 853,162 (1952).

78. J. U. White, J. Opt. Soc. Amer. 32, 285 (1942).

79. Reference 32.

80. D. C. Moule, C. R. Subramaniam, Can. J. Chem. 47, 1011 (1969).

81. M. J. Dewar, The Molecular Orbital Theory of Organic Chemistry, McGraw-Hill Book Co., N.Y. (1969).

82. G. W. Robinson in L. Marton: Methods of Experimental Physics, Vol. 3, p. 155 (1962).

83. J. H. Callomon, K. K. Innes, J. Molec. Spectrosc. 10, 166 (1963).

84. A. B. F. Duncan, E. H. House, private communication in Ref. (60).

85. G. W. King, A. A. G. van Putten, J. Molec. Spectrosc., to be published.

86. D. Chadwick, Can. J. Chem. 50, 737 (1972).

87. W. J. Balfour, Ph.D. Thesis, McMaster University, Hamilton (1967).

88. J. B. Coon, N. W. Naugle, R. D. McKenzie, J. Molec. Spectrosc., 20, 107 (1966).

APPENDIX A

DEVELOPMENT OF CNDO THEORY[65]

This investigator has used the CNDO (complete neglect of differential overlap) calculation to obtain eigenvalues and transition energies. No attempt was made to alter (in hopes of improving) the program. The following is the author's attempt to make the calculation less of a "black-box" calculation for himself. A more detailed treatment of the theory may be found in the literature[62,63,64].

The problem is one of solving for each electron:

$$H\phi = E\phi \qquad [A.1]$$

Minimum values of E are obtained by making use of the variation theorem[59]. One then obtains n equations of the type:

$$\sum_{\nu}^{n} H_{\mu\nu}C_{\nu} - \varepsilon \sum_{\nu}^{n} S_{\mu\nu}C_{\nu} = 0 \qquad [A.2]$$

or

$$\sum_{\mu}^{n}(H_{\mu\nu} - \varepsilon S_{\mu\nu})C_{\nu} = 0 \qquad [A.3]$$

For solutions to exist (other than the trivial solution), the determinant of the coefficients must be equal to zero.

Equation [A.3] can be transformed to matrix notation and will take the form:

$$\underset{\sim}{H}\,\underset{\sim}{C} = \underset{\sim}{S}\,\underset{\sim}{C}\,\underset{\sim}{\varepsilon} \qquad [A.4]$$

To facilitate the calculation two assumptions are made:

(i) the overlap integral is ignored unless the same centre is being considered; and

(ii) the terms of the H matrix are obtained empirically:

on the diagonal	$H_{\mu\nu} = \alpha$	coulomb integral	
off the diagonal	$H_{\mu\nu} = \beta$	if μ, ν are adjacent atoms	[A.5]
	$= o$	otherwise	

The major shortcoming of the theory developed to this point arises from the fact that the Hamiltonian H has not been clearly defined. The first and most important improvement then is to include electron repulsion in the Hamiltonian. The "effective" Hamiltonian thus becomes (for electron 1):

$$H_{eff} = -\frac{1}{2}\nabla_1^2 - \sum_{\alpha}\frac{Z_\alpha}{R_{\alpha 1}} + 2\sum_{j}^{occ}\frac{\phi_j^2(j)}{r_{ij}}d\tau_j \qquad [A.6]$$

where the second summation is carried out over all doubly occupied orbitals.

Equation [A.4] is more often written as:

$$\underset{\sim}{F}\,\underset{\sim}{C} = \underset{\sim}{S}\,\underset{\sim}{C}\,\underset{\sim}{\varepsilon} \qquad [A.7]$$

where $\underset{\sim}{F}$ is called the Fock matrix.

The F matrix contains terms:

$$F_{\mu\nu} = \int P_\mu(1)\, H_{eff}\, P_\nu(1)\, d\tau_1 \qquad [A.8]$$

In the evaluation of equation [A.7] several approximations in the CNDO method:

(i) the basis set is restricted to include only valence electrons, while the inner shell electrons are considered as a non-polarizable core;

(ii) in the equation $\underset{\sim}{F}\,\underset{\sim}{C} = \underset{\sim}{S}\,\underset{\sim}{C}\,\underset{\sim}{\varepsilon}$, the overlap matrix is replaced by the unit matrix;

(iii) the coulomb integrals are limited to one per atom pair, and this integral is taken as the average electronic repulsion between any electron on atom A and any electron on atom B; and

(iv) in the case of two-centre integrals:

$$\int P_\mu P_\nu P_\sigma P_\lambda d\tau = \delta_{\mu\nu}\delta_{\sigma\lambda}\int P_\mu P_\mu P_\lambda P_\lambda d\tau \qquad [A.9]$$

The CNDO programs used followed a self-consistent-field type development in that:

(i) an initial guess is made as to the molecular orbital coefficients,

$C_{\mu i}$, using a Hückel type calculation;

(ii) the electrons, in pairs, are fed into the molecular orbitals, starting with the lowest energy orbital;

(iii) a density matrix $P_{\mu\nu}$ ($P_{\mu\nu} = 2 \sum_{j}^{occ} C_{\sigma j} C_{\lambda j}$) is calculated using the coefficients of the occupied molecular orbitals, and then used to form a new Fock matrix - $F'_{\mu\nu}$; and

(iv) the diagonalization of $F'_{\mu\nu}$ leads to a set of first iterative coefficients - $C'_{\mu i}$.

The iterations are repeated until either the total energy (Pople-Dobosh program) or the orbital coefficients (Jaffé program) are consistent to within a predetermined accuracy.

The Pople-Dobosh program used Pariser-Parr[66] type repulsion integrals while the Jaffé program used Mataga-Nishimato[67] type integrals. The differences arising due to these two methods is discussed elsewhere[68,8].

Configuration Interaction[81]

Configuration interaction (CI) is introduced to allow for the electron correlation due to the mutual coulomb repulsion of the electrons. The total wave function is constructed as a linear combination of two or more Slater determinants[59] Φ_K:

$$\Psi = \sum_K A_K \Phi_K \qquad [A.10]$$

A_K's are chosen that lead to the lowest total energy. By using a sufficient number of different functions, Φ_K, the true wave function can be approached.

In the CNDO calculations, the basis set is a set of atomic orbitals which are equal in number to the total number of valence electrons (N say). N molecular orbitals result from the calculation. N/2 are required to accommodate the N electrons. This configuration of N electrons in the N/2 molecular orbitals of lowest energy is called the ground state determinant. Alternate

determinants Φ_K can be constructed by distributing the N electrons within the N molecular orbitals.

The main difficulty lies in the number of possible configurations that can be constructed from the set of molecular orbitals. However, if ground state wave functions are constructed, only lower energy configurations are likely to be important. Also it can be proven that singly excited configurations cannot be used to construct ψ, if the ground state is being considered.

In excited states, all singly excited configurations can combine and the interaction will be large. For a useful description of excited states, configuration interaction must be used.

APPENDIX B

EVALUATION OF THE ONE-CENTRE MOMENT INTEGRAL

2s - 2p

Assume $$\phi_{2s} = \left(\frac{Z^5}{96\pi}\right)^{1/2} r\, e^{-Zr/2}$$

$$\phi_{2p} = \left(\frac{Z^5}{32\pi}\right)^{1/2} r\, e^{-Zr/2}\cos\theta$$

where Z is the Slater coefficient.

Then $$\int \phi_{2s} |\tilde{M}| \phi_{2p} d\tau$$

Expressing the integral in terms of spherical polar co-ordinates:

$$\tilde{U} = \int_{r=0}^{\infty} \int_{\theta=0}^{\pi} \int_{\phi=0}^{2\pi} \left(\frac{Z^5}{96\pi}\right)^{1/2} r\, e^{-Zr/2} |e\tilde{r}| \left(\frac{Z^5}{32\pi}\right)^{1/2} r\, e^{-Zr/2}\cos\theta r^2 \sin\theta dr d\theta d\phi \quad [B.1.]$$

replace er by ercosθ, that is, consider z component,

since $$\int_0^{2\pi} k d\phi = 2\pi k \qquad (69) \qquad [B.2]$$

and $$\int_0^{\pi} \cos^2\theta \sin\theta d\theta = \frac{2}{3} \qquad (69) \qquad [B.3]$$

[B.1] reduces to

$$\tilde{U} = 2\pi \frac{2}{3} e \left(\frac{Z^5}{96\pi}\right)^{1/2} \left(\frac{Z^5}{32\pi}\right)^{1/2} \int_{r=0}^{\infty} r^5\, e^{-Zr} dr \qquad [B.4]$$

$$= 2\pi \frac{2}{3} e \left(\frac{Z^5}{96\pi}\right)^{1/2} \left(\frac{Z^5}{32\pi}\right)^{1/2} \frac{5!}{Z} \qquad [B.5]$$

If the integral considered is on carbon then[26]:

$$Z = 3.25$$

then [B.5] becomes:

$$\tilde{U} = \int \phi_{2s_C} |\tilde{M}| \phi_{2p_{z_C}} d\tau$$

$$= .888231$$

This number agrees exactly with the value quoted by Burnelle and Kranepool[51].

APPENDIX C

EVALUATION OF CARTESIAN DISPLACEMENT CO-ORDINATES

The cartesian displacement co-ordinates ξ are related to the normal co-ordinates Q by:

$$\xi = M^{-1}B'(L^{-1})'_{unsym}Q \qquad [C.1]$$

where M^{-1} is a diagonal matrix with elements equal to the reciprocal masses of the appropriate masses.

B' is the transpose of the B matrix. The B matrix is used to relate the symmetry co-ordinates S and the cartesian displacement co-ordinates:

$$S = B\xi \qquad [C.2]$$

$(L^{-1})'_{unsym}$ is the transpose of the L^{-1}_{unsym} matrix defined by:

$$Q = L^{-1}_{unsym}S \qquad [C.3]$$

Equation [C.1] can also be written as:

$$\xi = \left(\frac{\partial r_\sigma}{\partial Q_o}\right)_o Q \qquad [C.4]$$

Pople and Sidman[60] quote values of $\left(\frac{\partial r_\sigma}{\partial Q_o}\right)_o$ for H_2CO[70]. For $C\ell_2CS$, the matrix resulting from $M^{-1}B'(L^{-1})'_{unsym}$ was evaluated.

The unsymmeterized L matrix was obtained from the symmeterized L matrix using the following relations:

$$L_{unsym} = U^{-1}L_{sym} \qquad (71) \qquad [C.5]$$

The elements of the U matrix were taken from Overand and Scherer[71]. The elements of the unsymmeterized L matrix for in-plane vibrations were obtained from C. R. Subramaniam[72] and are listed in Table C.1.

The cartesian displacement co-ordinates for $C\ell_2CS$ are listed in Table

C.2, for the three asymmetric vibrations. The out-of-plane vibration was calculated separately using equation [C.1].

Table C.1

Unsymmeterized L Matrix for $C\ell_2CS$

	ν_1	ν_2	ν_3
Δr_{CS}	+.334369	+.051796	-.009882
$\Delta r_{CC\ell_1}$	-.159544	+.123679	+.008128
$\Delta r_{CC\ell_2}$	-.159544	+.123679	+.008128
$\Delta\theta_{C\ell_1CC\ell_2}$	+.248501	-.050171	+.170308
$\Delta\theta_{SCC\ell_1}$	-.124250	+.025085	-.085154
$\Delta\theta_{SCC\ell_2}$	-.124250	+.025085	-.085154

	ν_5	ν_6
Δr_{CS}	.000000	.000000
$\Delta r_{CC\ell_1}$	+.265418	+.025317
$\Delta r_{CC\ell_2}$	-.265418	-.025317
$\Delta\theta_{C\ell_1CC\ell_2}$	.000000	.000000
$\Delta\theta_{SCC\ell_1}$	+.257365	-.152717
$\Delta\theta_{SCC\ell_2}$	-.257365	+.152717

Table C.2

Cartesian Displacement Co-ordinates for $C\ell_2CS$

	Q_4 (b_1)	Q_5 (b_2)	Q_6 (b_2)
x_C	0.90	-0.22	0.00
y_C	0.00	0.58	0.00
z_C	0.00	0.00	-0.92
x_S	0.00	0.00	0.00
y_S	0.00	0.71	0.00
z_S	0.00	0.00	0.21
$x_{C\ell_1}$	-0.26	-0.26	0.00
$y_{C\ell_1}$	-0.18	-0.56	0.00
$z_{C\ell_1}$	0.00	0.00	0.17
$x_{C\ell_2}$	-0.26	-0.26	0.00
$y_{C\ell_2}$	+0.18	+0.56	0.00
$z_{C\ell_2}$	0.00	0.00	0.17

APPENDIX D

OBSERVED BANDS OF THE UNKNOWN SYSTEM

HIGH RESOLUTION

Measured from spectra recorded on the Ebert Spectrograph.

Frequency	Intensity[†]
30529.552	s
30540.550	vw
30755.013	w
30780.336	w
∿30810	vw
30902.724	w
30903.259	w
∿30984	vw
31100.900	w
31102.999	vw
31102.663	vw
31182.799	w
31191.151	vw
31197.466	w
31198.830	vs
31318.632	w
31334.627	vw
31336.813	w
31338.331	s
31339.553	w
31342.677	vs
31344.062	vs
31346.173	s
31348.827	s
31350.636	s
31352.877	s
31358.274	s
31384.686	vw

Frequency	Intensity[†]
31397.728	vw
31400.829	vw
31413.075	w
31422.374	w
31422.895	vw
31517.822	w
31526.789	s
31535.389	s
31541.086	w
31543.496	w
31545.264	vw
31549.456	w
31559.832	s
31583.765	vw
31606.283	w
31607.048	w
31618.979	vw
31619.689	vw
31620.347	vw
31688.809	vw
31695.900	w
31705.441	vw
31723.082	w
31726.443	w
31741.818	w
31754.691	w
31775.591	w
31776.822	w
31782.877	vw
31783.613	vw
31789.299	s
31792.227	s
31795.383	s
31806.168	w

Frequency	Intensity[†]
31806.842	w
31809.811	w
31857.974	w
31861.978	vw
31863.539	vw
31863.465	vw
31879.765	vw
31885.509	vw
31951.177	w
31975.181	vs
31977.302	w
31982.302	vw
31982.847	vw
31983.629	vw
31985.731	vw
31997.840	w
31997.205	w
32010.068	w
32011.009	vw
32020.921	s
32023.663	vw
32025.148	vw
32049.314	vw
32056.688	w
32071.849	vs
32083.083	w
32236.636	w
32239.232	s
32242.173	w
32242.943	w
32250.147	w
32251.027	s
32319.583	w
32321.674	w
32327.057	w

Frequency	Intensity[†]
32371.568	w
32446.380	w
32450.251	w
32451.190	s
32510.423	vw
32528.864	vw
32530.449	vw
32532.606	vw
32533.926	vw
32540.743	w
32542.026	vw
32543.082	vw
32556.239	vw
32573.667	w
32647.725	vw
32701.217	vw
32703.227	w
32746.432	vw
32749.426	vw
32752.269	vw

[†]vs very strong
s strong
w weak
vw very weak

APPENDIX E

OBSERVED BANDS OF THE UNKNOWN SYSTEM

LOW RESOLUTION

Measured from spectra recorded on the Bausch and Lomb Model 11.

Frequency	Intensity[†]
30554	s
30525	vs
30468	s
30447	s
30436	s
30419	w (29775 + 644)
30405	w (29762 + 643)
30384	s
30368	s
30352	s
30345	s
30324	w
30275	s
30265	vs
30256	vs
30241	s (29601 + 640)
30215	s
30195	w
30180	w
30087	vs (29449 + 638)
30056	s
30044	s
29983	w
29948	s (30419 - ν_4'')
29925	s (30215 - ν_3'')
29899	s
29874	s (29232 + 642)
29864	s

Frequency	Intensity†
29849	s
29839	s (30345 - ν_2'')
29786	s
29775	s (30275 - ν_2'')(29134 + 641)
29762	s (29121 + 641)
29718	s (30215 - ν_2'')
29695	s
29674	s
29669	s (29030 + 639)
29655	s
29631	w
29609	w
29601	w (30419 - ν_5'')
29509	w (30324 - ν_5'')
29500	s (29786 - ν_3'')
29480	s
29465	w
29449	w (29948 - ν_2'')
29442	w
29423	vw (29925 - ν_2'')(28783 + 640)
29410	vw
29407	vw (29874 - ν_4'')(29695 - ν_3'')(28764 + 643)
29374	w (29874 - ν_2'')(29849 - ν_4'')
29365	w (29864 - ν_2'')(29839 - ν_4'')(29655 - ν_3'')
29356	w
29349	w (29849 - ν_2'')
29335	w (29839 - ν_2'')
29293	vw (29762 - ν_4'')
29279	w (29786 - ν_2'')(30419 - ν_1'')
29259	vw (29762 - ν_2'')
29232	s (30368 - ν_1'')
29219	w (29718 - ν_2'')
29148	w
29134	w (29948-ν_5'')(29655-ν_2'')(29601-ν_4'')(30275-ν_1'')

Frequency	Intensity[†]
29121	w
29083	s (29899 - ν_5'')
29071	s
29053	vw (29874 - ν_5'')
29030	vw (29849 - ν_5'')(29550 - ν_4'')
29015	w
28993	vw (29465 - ν_4'')(29500 - ν_2'')(29239 - ν_3'')
28958	w (29465 - ν_2'')(29775 - ν_5'')
28926	w
28856	s (29695 - ν_1'')(29674 - ν_5'')(29669 - ν_5'')
28807	s (29948 - ν_1'')
28783	s (29071 - ν_3'')
28764	vw (29899 - ν_1'')(29053 - ν_3'')
28634	w (29775 - ν_1'')
28629	w (29449 - ν_5'')
28618	w
28569	w (29071 - ν_2'')
28556	w
28545	w
28537	s (29674 - ν_1'')
28490	w
28414	w
28409	s
28268	w
28252	w (29071 - ν_5'')
28199	w (28490 - ν_3'')
28146	s
27957	w

[†] s strong
w weak
vw very weak